Ceramic Heads in Total Hip Replacements:

Surgical Impaction Force and Retrieved Implant Damage Assessment

BY

KIRSTEN T SIPEK
B.S., University of Wisconsin-Milwaukee, 2016

THESIS
Submitted as partial fulfillment of the requirements
for the degree of Master of Science in Bioengineering
in the Graduate College of the
University of Illinois at Chicago, 2019

Chicago, Illinois

Defense Committee:

Mathew Mathew, Chair and Advisor

Robin Pourzal, Co-Advisor, Rush University Medical Center

Hannah Lundberg, Bioengineering

ACKNOWLEDGEMENTS

I would like to thank my thesis committee from the University of Illinois at Chicago and Rush University Medical Center- Dr. Mathew Mathew, Dr. Robin Pourzal, and Dr. Hannah Lundberg- for their support and mentorship. Especially Dr. Pourzal who guided me through this project and assisted me in every step. I would also like to thank Dr. Jonathan Gustafson, Stephanie McCarthy, and Deborah Hall for their support and expertise on the varying aspects of this project. The UIC Machine Shop was instrumental in in designing and assembly the testing set-up. I appreciate the surgeons that participated in the study and Dr. Brett Levine's input in designing a set-up to accurately represent what occurs in the operating room.

TABLE OF CONTENTS

TABLE OF CONTENTS

LIST OF TABLES

TABLE PAGE

LIST OF FIGURES

FIGURE PAGE

LIST OF ABBREVIATIONS

CAD	Computer Aided Drafting
CoCrMo	Cobalt Chromium Molybdenum
SEM	Scanning Electron Microscope
THR	Total Hip Replacement
TiAlNb	Titanium Aluminum Niobium
TiAlV	Titanium Aluminum Vanadium

SUMMARY

Corrosion in total hip replacements (THR) is an ongoing occurrence, creating a need for additional revision surgeries. Ceramic femoral heads are becoming a more popular choice, but the failure modes and assembly techniques are not thoroughly researched. This study had two purposes: 1. To determine surgical impaction force applied to metal and ceramic total hip replacements; 2. To characterize damage features of retrieved ceramic heads.

The results of aim 1 were also analyzed with respect to surgeon experience level—attending, fellows, and resident clinicians—of the 32 participants and the off-axis impaction angle. Surgeons assembled both a ceramic and metal head onto a 12/14 stem taper attached to a 3-dimensional force sensor (9347C, Kistler® USA, Amherst, NY). A benchtop testing apparatus was developed and employed to simulate the operating room procedure for total hip modular junction assembly. The second aim consisted of analyzing surface damage features of 25 retrieved ceramic head hip implants using the RedLux Metrology Optical Coordinate Measuring Machine (Ortholux, RedLux, Ltd, Romsey, UK) as well as a scanning electron microscope and Zygo 3D Optical Surface Profiler (Zygo Corporation, Middlefield, CT).

The results from the surgeon-applied impaction study showed no significant differences between the forces applied to metal and ceramic heads—contrary to our initial hypothesis. Interestingly, attending surgeons applied the greatest forces regardless of the head taper material and demonstrated the lowest variability among the surgeon groups. The attending surgeons also demonstrated the smallest off-axis impaction angle, indicating more “accurate” assembly of the head taper onto the stem taper. Results from the retrieved ceramic head implants indicated evidence of fretting, granular, and crevice corrosion on the stem tapers. There were also observations of plastic deformation and material transfer that could indicate a well-bonded head and stem interface.

These studies indicate that there is no continuity among surgical impaction technique, but attendings had the least variability with regards to force and off-axis angle. Hip implants with ceramic heads still have incidences of corrosion at the head-stem interface as well as evidence of material transfer onto the femoral head taper. It is important that surgeons impact the femoral head with a great enough force to create a strong bond and lessen the possibility of corrosion and component loosening.

1 INTRODUCTION

(Parts of this chapter were previously published as D'Antonio, J.A., Capello, W.N., and Naughton, M. (2012). Ceramic Bearings for Total Hip Arthroplasty Have High Survivorship at 10 Years. Clin. Orthop. Relat. Res. *470*, 373. And as Uchiyama, K., Inoue, G., Takahira, N., and Takaso, M. (2017). Revision total hip arthroplasty - Salvage procedures using bone allografts in Japan. J. Orthop. Sci. Off. J. Jpn. Orthop. Assoc. *22*, 593–600.)

1.1 Background

Total hip replacements (THR) have been an effective treatment choice for arthritis and other disorders for over a century. The first attempt at a hip replacement occurred in Germany in 1891. The modern, low friction arthroplasty, on which current devices are based, was invented by Sir John Charnley in the early 1960's (Knight et al., 2011). As more knowledge and experience was gained, there have been modifications to improve the functionality and lifespan of hip implants. This involved the use of ceramics in the femoral head and acetabular liner.

During total hip replacement, the femur is hollowed out to insert a metal stem (Figure 1a (Uchiyama et al., 2017)). Then, the femoral head and acetabulum are also replaced. The femoral head and stem junction can be replaced with a metal-on-metal or metal-on-ceramic interface. The acetabulum is replaced with a metal cup and either a polyethylene or ceramic liner. Figure 1b (D'Antonio et al., 2012) shows the varying femoral head and acetabular components. System I and System II show a ceramic femoral head paired with a ceramic acetabular liner. System III shows a metal femoral head and a polyethylene acetabular liner.

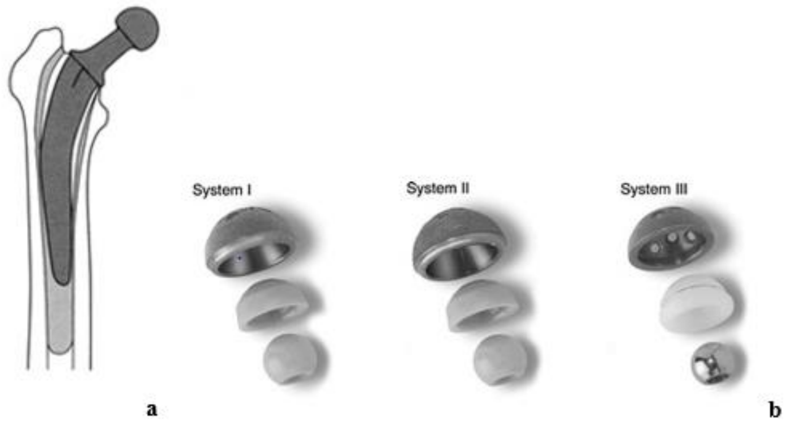

Figure 1: a) THR stem component(Uchiyama et al., 2017) b)THR femoral head and acetabular components(D'Antonio et al., 2012)

Most total hip replacements use modularity between the head and stem of the implant which allows the surgeon to best fit the implant to specific patient anatomy. In some cases, micromotion within the head-stem taper junction can lead to fretting corrosion and ultimately, implant failure. Over the last few years, there has been an increase in implant failure due to adverse local tissue reactions from fretting (Cooper et al., 2013). The onset of micromotion is partially related to the assembly of the head onto the stem by the surgeon. The load applied by the surgeon drives the contact mechanics and how well these two components bond together. Depending on the surgical approach and patient anatomy, the surgeon may not be able to apply the load directly in line with the taper axis. There are different implant assembly techniques such as, load applied, number of hammer strikes, and the surgeon's chosen approach. These are all dependent on the surgeon's experience level and the training they have received. In order to decrease the risk of corrosion, more surgeons are using chemically inert ceramic heads instead of Cobalt Chromium Molybdenum (CoCrMo) alloy metal heads (AJRR, Fifth Annual Report, 2018). However, there are unknown potential consequences with the ceramic heads, such as, fracture and surface fatigue. Because ceramic heads are still paired with metal stems and/or metal sleeves, there is still a risk of corrosion. It is unknown whether surgeons assemble the ceramic femoral heads with less load due to the possibility of fracture. Without a significant enough impaction force, the patient could be more likely to experience implant failure due to loosening and corrosion. Because of this, it is important to study whether surgeons are using a great enough force to implant the prosthesis.

1.2 Purpose

1.2.1 Aim 1: Determination of Impaction Forces

The first aim of this study was to determine the force applied by surgeons in assembling the femoral head onto the stem taper. The impaction force used for a metal femoral head will be compared to that of a ceramic femoral head. We hypothesize that surgeons will apply less force when impacting ceramic heads as compared to metal heads. Physicians from every level of education from Rush University Medical Center (Chicago, IL) will be involved in the study, which will demonstrate how the implantation technique varies not only among experience, but also between surgeons of the same level. This will establish if there is a lack of continuity throughout surgical training and education with regards to hip implantation.

1.2.2 Aim 2: Assessment of Damage Features on Ceramic Head Tapers and Corresponding Trunnions

The purpose of this aim was to analyze the damage and wear patterns of 25 retrieved ceramic hip implants. We hypothesize that the ceramic heads will lead to less damage, and there may be an increase in material transfer. Each component of the implant will be studied, including the head, head taper, and stem taper, using scanning electron microscopy and surface topography analysis. By doing so, the wear patterns and most affected areas can be found.

2 LITERATURE REVIEW

2.1 Role of Impaction Force on Subsequent Damage Processes

2.1.1 Wear and Corrosion

Fretting and crevice corrosion commonly occur in hip implants due to bodily fluids entering the junction between the stem taper and femoral head. Fretting corrosion is produced by micromotions between the implant components during cyclic loading. Crevice corrosion stems from the repassivation of the oxide layer on the metal surface (Hallab et al., 2004). Corrosion at the head-stem taper junction has been seen in nearly all retrieved hip implants, with severe corrosion occurring in 31% (Hothi et al., 2016). With the high prevalence of hip implant corrosion, it is important to investigate possible causes, such as impaction load and assembly variability. Both English and Haschke completed similar studies in which the optimal impaction load to decrease taper damage and fretting was determined using varying loads. Forces of 2 kN, 4 kN, 6 kN, and 8 kN were investigated. These values were determined based on average surgical impaction force being slightly over 4 kN as well as utilizing clinical observations (Haschke et al., 2016). The blows were delivered using a drop hammer, and all components involved were either Cobalt Chromium or Titanium. There was a force sensor under the drop weight to ensure correct loading. The seating distance of the head, which describes how far the taper is inserted, was measured and compared for the differing load values. In addition, Haschke determined the amount of micromotion after 2000 loading cycles. The results indicated that greater loads led to a greater seating distance, meaning a more engaged head-taper interface. It was found that the higher assembly loads significantly reduced the amount of micromotion between the head and taper. These analyses indicate that a higher impact assembly leads to improved initial and future outcomes of the hip implant and a reduced probability of wear and corrosion. However, it is unknown how surgeons assemble the head onto the taper in the operating room, as these studies utilized a benchtop setup. English also simulated the average hip loading over 10 years using Finite Element Analysis, at which 1 million walking cycles per year was estimated (English et al., 2016). The results suggest that an increased impaction force leads to less fretting wear over time, with the optimal load being 6 kN. With greater loading, less fretting corrosion is present, but there is an increased risk of taper deformation. These results will serve as a guideline for how well the surgeons assemble the implant to prevent fretting corrosion. However, ceramic heads were not involved in the studies and may require different loading based on the fit and material interaction.

The magnitude of impaction assembly force is not the only factor in optimal taper seating. Because surgeons in the operating room are not able to perfectly apply on-axis loads, off-axis forces are an important consideration as well. In a related study, off-axis forces during impaction were analyzed and their influence was determined(Frisch et al., 2016). Implants were assembled utilizing a drop hammer with load cells in the hammer and at the head-neck junction. Loads were applied on-axis as well as off-axis to determine any positive or negative effects. The off-axis impacts were located 10° off-axis in varying directions. Also, the tapers were angled at 0°, 8°, and 15° to establish which provided the greatest implant stability. Based on the force transmitted to the taper, axial impaction was best for necks at a 0° angle. However, off-axis impaction provided better loading for necks angled at 8° and 15°. For the most optimal assembly, surgeons need to determine the implant angle and adjust their approach based on that information. This thesis will incorporate loads applied directly by surgeons, rather than a drop hammer, as well as calculation of off-axis forces in both the vertical and horizontal directions.

2.1.2 Pull-Off Force

Pull-off force is the current standard for indicating how well the head and stem of the implant fit together. Three studies investigated how the impaction force and number of blows affected the pull-off force of the head. All the investigations utilized a drop hammer to apply the impaction. Heiney had the resident and attending surgeons hit on pressure sensitive Fuji film and then translated that load to a drop hammer mechanism (Heiney et al., 2009). None of the studies had surgeons simulate surgery with a stem taper and femoral head setup, limiting the clinical applicability of these results. Danoff studied whether a 6 kN or 14 kN load would create a greater pull-off force while also looking at the difference between one and two blows applied (Danoff et al., 2018). All studies indicate that the greater impaction results in a greater pull-off force. The studies related to impaction force measurement did not angle the taper to mimic the surgical environment. Each test places the taper on a flat, horizontal surface with the force being applied directly on top through the z-axis.

There is no standard hip implant assembly procedure for surgeons to follow which leads to a variability in technique. This is also true for the number of blows applied to the femoral head during impaction. Researchers investigated the effect multiple blows has on the bond strength and the head-stem taper junction. Rehmer and Danoff state that multiple blows did not affect pull-off force, while Heiney suggests it did (Rehmer et al., 2012). Heiney's results indicated that the head needed to be impacted at least twice to create a bond with the stem taper. The presence of this bond can decrease the likelihood of micromotion and fretting corrosion. The current thesis will compare surgical assembly technique among varying experience levels, including the number of blows applied by each surgeon.

2.2 Ceramic Heads

2.2.1 History of Ceramic Heads in Total Hip Replacement

To combat the concerns of wear and friction, Pierre Boutin introduced the first ceramic-on-ceramic hip implant in 1970 (Knight et al., 2011). These were best suited for active, young patients due to the resistance to wear and low friction. Before becoming a more prevalent choice in the United States in recent years, ceramic implants were more commonly utilized in Europe.

With the increased use of ceramic-on-ceramic, the disadvantages and failure modes became more apparent. These included producing a squeaking noise during movement as well as a greater possibility of fracture. Hip implants with ceramic heads are most often paired with a highly cross-linked polyethylene acetabular liner to reduce wear particles and wear rates. However, the advent of Biolox forte and Biolox delta may revitalize the use of ceramic-on-ceramic because of the lowered fracture risk (Lehil and Bozic, 2014). Biolox forte was created with the use of hot isostatic pressure to increase the density of the ceramic and limit fracture (Ma and Rainforth, 2012). The use of Biolox delta ceramic began when the Biolox forte ceramic heads experienced stripe wear after removal due to loosening. This new material was an alumina ceramic nanocomposite that created a tougher surface and has been used successfully in recent years. Failure modes of ceramic head implants have not been thoroughly researched because it takes time in-vivo for implants to fail. Retrieval studies are just beginning to see these failure paths.

2.2.2 Metal vs. Ceramic: Advantages and Disadvantages

Looking at both ceramic and CoCr heads, Kurtz found that the ceramic heads had lower fretting and corrosion scores (Kurtz et al., 2013). The study also demonstrated that ceramic heads had only positive taper angle clearance which results in proximal contact between the head and taper. The positive taper angle in ceramic heads is important to minimize the potential for fracture, as a proximal contact allows for maximal seating depth of the head taper onto the stem taper. The proximal contact location was further verified by the location of metal markings on the interior head surface. Kurtz's conclusion that ceramic heads had lower corrosion scores is inconsistent with that of Di Laura who did not determine a difference in CoCr stem corrosion between ceramic and CoCr heads (Di Laura et al., 2017). However, there was less material loss in the stem for the ceramic heads when compared to metal heads. Utilizing the scanning electron microscope and RedLux profiler will allow study of the stem surface as well as the interior head surface. Topographical analysis will determine if there is material loss, corrosion, or material transfer.

Contaminants between the head and stem taper surfaces can lead to implant failure or loosening. For ceramic heads, both static loading and cyclic loading were applied with and without the presence of contaminants, and the metal markings were observed (Valet et al., 2014). The static loading involved a hammer blow, as seen in implant assembly. The force was no greater than 46kN, and no less than 20kN. Cyclic loading occurred at 4kN loading for 10 million cycles. The contaminants introduced were blood and bone chips. Results indicated that the presence of contaminants caused asymmetrical metal markings on the interior head surface. No contaminant resulted in symmetrical metal markings for both statically and cyclically loaded heads.

A study of ceramic-on-ceramic hip implants looked at the probable causes of squeaking after a hip replacement (Restrepo et al., 2008). This did not correlate with any instability or pain as reported by the patients. The common observations during revision surgery of 6 squeaking hips included rim impingement, stripe wear, and metal transfer. The rim impingement is evidenced by an indentation on the edge of the metal acetabular cup, and stripe wear is caused by edge loading. All revised implants had indication of stripe wear. However, more samples are needed to verify a correlation between stripe wear and implant squeaking. A case study was completed to observe the possible clinical outcomes from metal streaking that can occur during surgery (Tomek et al., 2012). The metal transfer streaks on ceramic heads can happen during surgery as the head is being placed into the liner, or due to in vivo dislocation.

A retrieval study viewed both ceramic and metal heads to determine if taper angle clearance can lead to fretting corrosion (Kocagöz et al., 2013). A total of 50 ceramic heads and 50 metal heads were used in this study. The taper angle clearance was measured, and surface topography analyzed for the heads as well as the stem tapers. From the measurements, the ceramic heads all exhibited proximal contact of the taper, meaning the taper is in contact with the proximal portion of the head taper. The metal femoral heads had both proximal and distal contact. While there was evidence of material transfer, none of the femoral heads demonstrated a correlation between taper angle clearance and fretting corrosion. However, on the metal heads, there was a relationship between fretting and eventual material loss, as viewed by scanning electron microscopy. Overall, this retrieval study provides insight and background into surface material markings but does not image the trunnions as will be done in the current study.

3 METHODOLOGY

3.1 Aim 1

3.1.1 Impaction Test Set-up

Utilizing previous works and literature, an impaction force testing apparatus was designed using AutoCAD (Autodesk, Inc., San Rafael, CA) with input from staff of the University of Illinois at Chicago Machine Shop. One of the requirements for the impaction force testing apparatus was to incorporate a 3-dimensional (3D) force sensor (9347C, Kistler® USA, Amherst, NY) to allow for measurement of the complex, 3D forces applied by surgeons. The first step in developing the testing apparatus was to obtain the CAD drawings of the force sensor in order to create a taper attachment and base plate that would secure to the force sensor. These drawings were obtained from the Kistler website product catalog. The CAD design for the 3D force sensor was used to design an interface between the force sensor and a manufactured stem taper. The initial design with the Kistler force sensor, stem taper, femoral head, impactor, and hammer is illustrated in Figure 2.

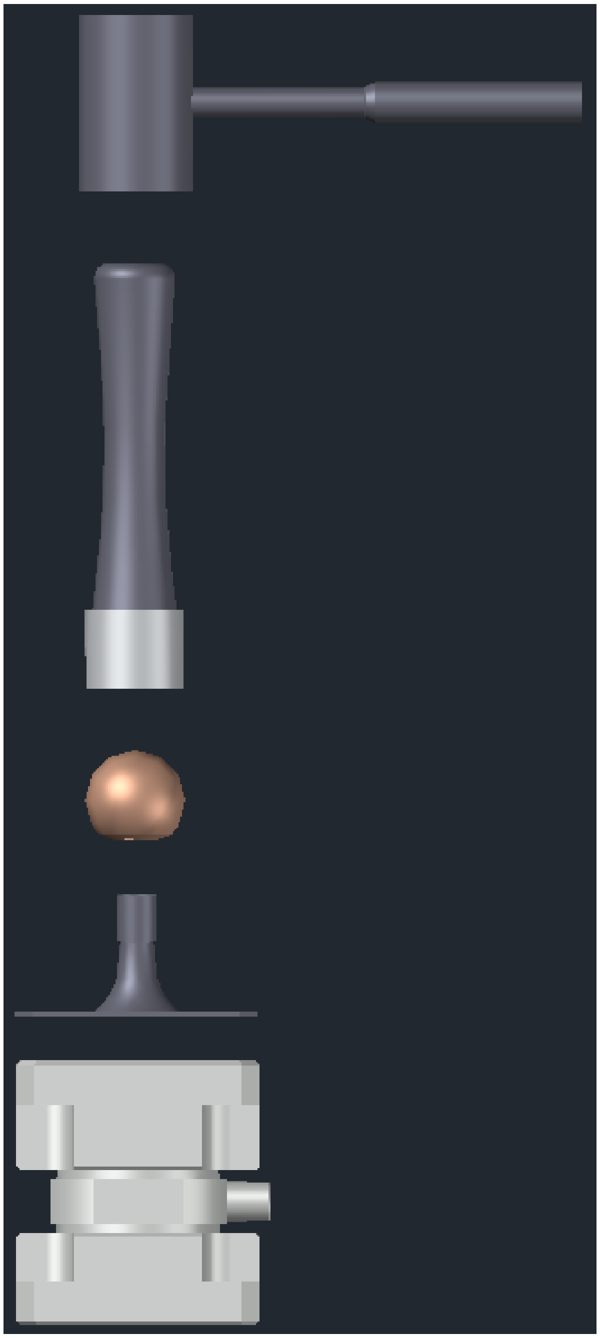

Figure 2: AutoCAD drawing of setup including force sensor, stem taper, head, impactor, and hammer

Once an initial design was drafted, the testing apparatus was critically assessed with machinists from the UIC machine shop. After consulting with orthopedic surgeon, Dr. Brett Levine, it was determined that the set-up should be elevated from the table, and the taper should be angled between 30° and 45° from horizontal. These parameters allow for the most realistic replication of hip replacement surgery. We discussed possible designs to angle the taper that would be repeatable for each surgeon. The first iteration consisted of two plates, each with a center angle. One angle had two holes and the other had one hole. These two plates would be hinged together, and a rod inserted in each plate setting it at either 30° or 45°, as shown on the left side of Figure 3. After some discussion, it was determined that the rod in this design could fail in shear, so the machine shop suggested a rigid angle plate already set at either 30° or 45° as shown on the right side of Figure 3. After considering the cost and inconvenience of two angle plates, a varying angle plate with an attached protractor was decided upon. This angle plate will ensure a consistent angle for each surgeon. The machinists developed a base plate that would fasten to the angle plate and screw into the force sensor to create a secure attachment.

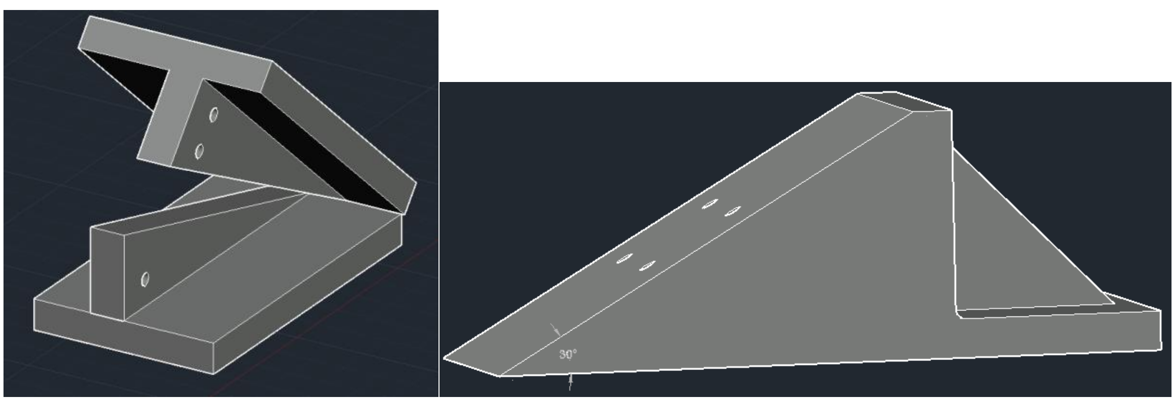

Figure 3: First iterations of angle plate design in AutoCAD

Following several design iterations, which included increasing the thickness of the taper base plate (Figure 4) as well as including a varying angle plate (Figure 5b), a final testing apparatus was built. This design consisted of a stainless-steel stem taper attached to a base plate that could be screwed directly into the force sensor. The taper was modeled after the precise measurements of a 12/14 stem taper.

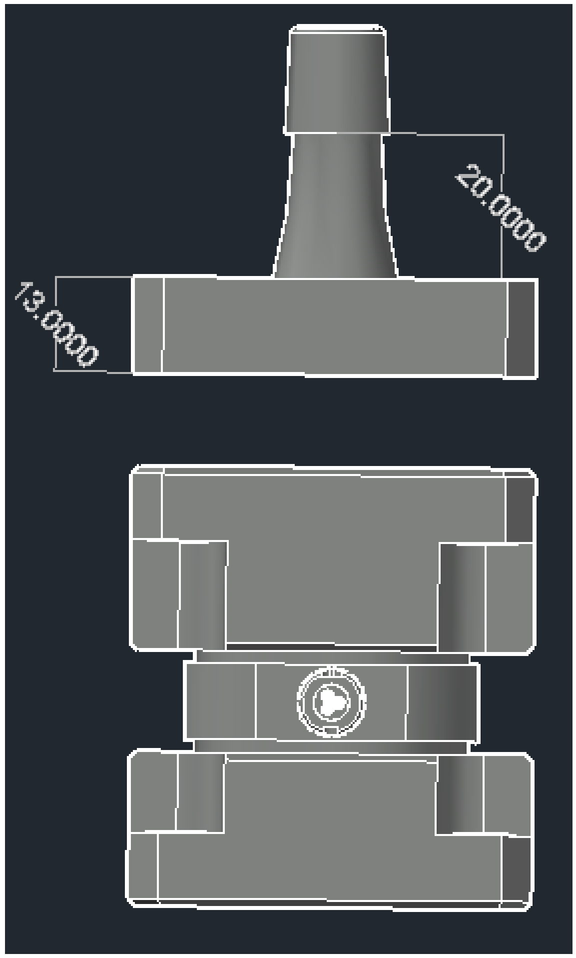

Figure 4: Final dimensioned taper and base plate

To the set-up, an elevated base was added to raise the taper 12 inches above the table. To secure the apparatus, industrial clamps were used, and the set-up was draped to allow visualization of only the taper and head, as done in surgery. The testing apparatus was designed to simulate the operating room environment and ensure repeatability across multiple tests. The final set-up is displayed in Figure 5. To collect the Fz, Fx, and Fy force data, the Kistler Force Link 9347C was connected to a Kistler LabAmp (5167A, Kistler® USA, Amherst, NY), an amplifier used to process the input force signal being measured by the force sensor. The collected 3D forces were recorded and stored using the Kistler web interface.

Figure 5: a) Elevated test set-up with taper, force sensor, and angle plate. b) Varying angle plate. c) 3-dimensional force sensor (Kistler 9347C) with taper and femoral head components

3.1.2 Impaction Data Collection

To begin the collection process, a surgeon data sheet was created to be used during testing. It included information such as surgeon name, experience level, right or left handed, and number of hip replacements performed. Surgeons were randomized to using either the ceramic or metal femoral head for their first visit. An example of this data sheet is shown in Table 1.

Sub ID#	Surgeon Name	Date Testing	Years Exp	# Hips Replaced	R/L Handed	Ask # Hits	Actual # Hits	Pressfit (Y/N)	Apply Pre-Load	Group (M vs C)	Notes
HT-01										M	
HT-02										M	
HT-03										M	
HT-04										C	
HT-05										M	
HT-06										M	
HT-07										C	
HT-08										M	
HT-09										M	
HT-10										M	
HT-11										M	
HT-12										M	
HT-13										M	
HT-14										C	
HT-15										M	
HT-16										C	
HT-17										C	
HT-18										M	
HT-19										C	
HT-20										M	
HT-21										M	
HT-22										C	
HT-23										C	
HT-24										C	
HT-25										M	
HT-26										C	
HT-27										C	

Table 1: Sample surgeon data sheet

Each surgeon was brought in and asked their name, the number of hips replaced, and if they were right or left handed. Experience level was categorized as follows: attending, fellow, resident. For the residents, the year in their program was also denoted. The randomized group M vs C indicated whether the surgeon would assemble a metal or ceramic head, respectively. The remaining categories on the questionnaire were completed as observations. A pre-load was defined as whether the surgeon lightly tapped the head prior to impaction in order to line up the strike. The number of strikes used for each trial was recorded as well as if the surgeon pressfit the head onto the taper before beginning impaction. Each participant was instructed to assemble the head onto the taper using their preferred surgical technique. After each assembly, the head was removed, and the surgeon was asked to assemble it again. This procedure was repeated for a total of 5 trials. The second visit occurred after at least 4 weeks of time. Testing was conducted in the same manner as described above in the first testing session, with the surgeons assembling the femoral head of opposite material as the first round. The CoCrMo head was 32 mm, and the ceramic head was 28 mm in diameter. During testing, any comments made by the surgeons regarding the accuracy of the set-up were recorded in the "Notes" section of the data sheet. These recommendations allowed us to understand the varying techniques or impaction equipment that physicians use and how to modify the set-up for future studies. At the conclusion of testing, each surgeon was asked to complete an exit questionnaire about the study. The questionnaire inquired about how surgeons assemble the femoral head onto the taper, with regards to force and type of approach. It also asked the surgeons about which material they believe has greater fracture resistance, and if the force can affect the success of the implant. The first question discussed whether the surgeons felt that the benchtop test setup accurately replicated what is done in the operating room. The answers were recorded using only subject ID as to ensure anonymity. This questionnaire (Figure 6) can assess how surgeons perceive the material strengths of metal and ceramic and how this may affect the force applied during impaction.

Date: ______________ Subject ID: __HT - ________

Rush Department of Orthopedic Surgery

Hip Taper Assembly Project: Surgeon Questionnaire

1. Do you feel that the testing setup accurately replicated the surgical environment?
   a. Yes
   b. No
   c. Somewhat

2. What is the primary approach you use during primary THA?
   a. Posterior
   b. Anterior
   c. Anterolateral
   d. Direct Lateral
   e. Other

3. Do you believe that the impaction force can affect the success of the hip implant?
   a. Yes
   b. No

4. Do you believe the number of assembly strikes can affect the success of the hip implant?
   a. Yes
   b. No

5. When attaching the femoral head to the stem, do you impact the femoral head directly and inline with the stem?
   a. Always
   b. Sometimes
   c. Rarely
   d. Never

6. Do you ever sacrifice the force of impaction to make sure you do not fracture the proximal femur?
   a. Always
   b. Sometimes
   c. Rarely
   d. Never

7. Which femoral head material do you think has the greatest fracture resistance?
   a. Metal
   b. Ceramic
   c. They're Equal

8. Compared to a metal head, how much force do you apply to the ceramic head during assembly?
   a. More force
   b. Less force
   c. Same force

Figure 6: Sample exit questionnaire

3.1.3 **Impaction Data Processing**

The majority of the data processing was completed utilizing MatLab R2017a (The MathWorks, Inc., Natick, MA) and Microsoft Excel (Microsoft, Redmond, WA). To begin, each subject's impaction data was imported into MatLab and then displayed on a graph. The graph showed the force (kN) in the Z direction on the vertical axis, with time on the horizontal axis. The coordinate system for representing the force data followed the system convention of the force sensor, with the Z direction defined as positive going into the taper, the positive X direction pointing downward, and the positive Y direction was to the right, as represented in Figure 7a.

Each strike appeared as a peak in the data, which was able to be isolated and the peak force determined. The corresponding peak forces in the off-axis directions, X and Y, were also calculated. Across the five trials, the average of the maximum forces was calculated, and these averages were utilized for data analysis as well as statistical calculations.

Standard deviations were calculated for each surgeon as well as across surgeons of the same experience level. This allowed for analysis of which grouping is the most consistent with the expectation being more experience equates to more consistency. To assess the ability of the surgeons to apply a force oriented along the stem taper axis (Z-axis), the off-axis angle, θz, was calculated as depicted in Figure 7b. This angle was calculated using the formula:

$$\theta z = \cos^{-1} \frac{Fz}{F} \tag{1}$$

where Fz is the force along the Z-axis, and F is the resultant force. A statistical analysis was completed, using a t-test, comparing the average peak force in the X, Y, and Z directions between metal and ceramic femoral heads. These force values were also analyzed with respect to surgeon experience level. The off-axis impaction angle (θz) was evaluated based on head material and surgeon experience level.

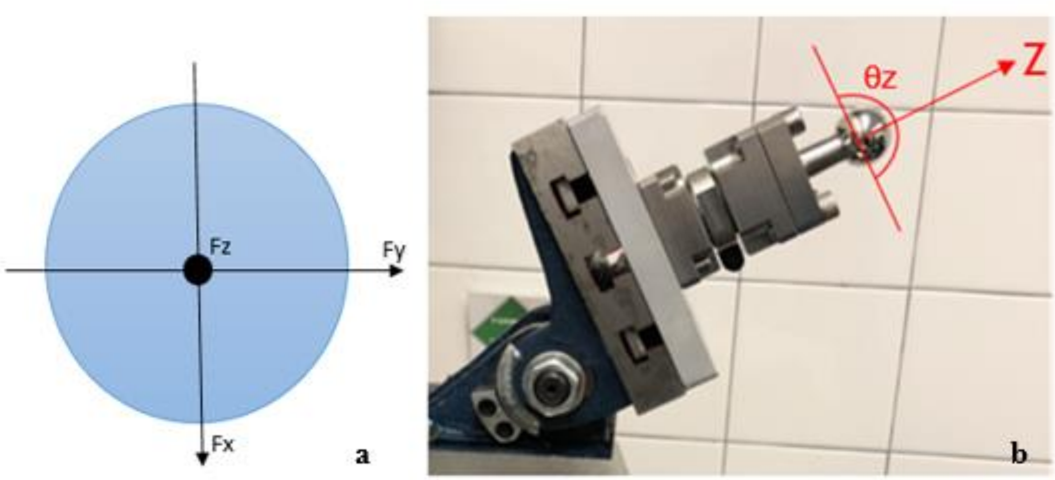

Figure 7: a) Impaction coordinates b) Off-axis impaction angle

3.2 <u>Aim 2</u>

3.2.1 <u>Metrology Optical Coordinate Measuring Machine</u>

Aim 2 of the study was to assess damage features and locations on the components of retrieved ceramic hip implants. To evaluate this aim, 25 retrieved ceramic head hip implants were collected, ensuring that each implant had a stem component. Of the 25 retrieved implants, 4 of them also had metal sleeves that attached to the stem taper. The first step was to confirm that all the ceramic heads were cleaned of debris and bodily fluids. To do this, each femoral head was rinsed under warm water while being brushed with a soft bristle toothbrush and allowed to air dry. Once all the heads were cleaned, each one was placed in the RedLux Metrology Optical Coordinate Measuring Machine (Ortholux, RedLux, Ltd, Romsey, UK) for surface measurement to assess surface damage such as metal streaking, or areas of corrosion. To measure the interior head surface, each femoral head taper was molded using Microset. Each stem taper was cut from the femoral stem component and attached to a dowel rod to allow for placement in the RedLux measurement machine. All stem tapers were measured for signs of material loss or surgeon damage. A unique aspect of the advanced taper surface characterization techniques employed in the current study is the ability to match the damage features on the stem taper with those on the head tapers to look for locations with the most contact wear and if there was evidence of loosening or corrosion. For implants with metal sleeves, the insides of the sleeves were molded in addition to the outside surface being measured, which would aid in identifying the type of contact between the stem taper and the sleeve as well as between the sleeve and the femoral head. After being scanned in the Redlux system, each stem taper and head taper were unwrapped utilizing the RedLux Profiler software which acted as a map to then complete surface analysis using the scanning electron microscope (SEM) and Zygo 3D Optical Surface Profiler (Zygo Corporation, Middlefield, CT) machines.

3.2.2 Surface Analysis (Scanning Electron Microscopy/Zygo)

Each cut stem taper was further assessed using the surface profiler (Zygo). The taper was initially aligned with undamaged regions in view to provide a reference for comparison to the damaged surfaces to determine how much and what type of damage occurred. The implants with metal sleeves were also imaged using the Zygo to see the initial machined surfaces. From these scans, the average machining line height and spacing were determined for each stem taper using MatLab.

For the 25 retrieved implants, stem tapers were viewed and evaluated for damage using a scoring-based system developed by Goldberg (Goldberg et al., 2002). Depending on the severity of the damage, each taper was visually scored from 1 to 4, with a score of 4 indicating large areas of corrosion damage. Table 2 below summarizes the data from the 25 implants. Included are the stem material and head material for each retrieved implant. The different stem materials include Cobalt Chromium Molybdenum (CoCrMo), Titanium Aluminum Vanadium (TiAlV), Titanium Aluminum Niobium (TiAlNb), and TMZF, a titanium alloy specific to Stryker (Stryker Orthopedics, Mahwah, NJ) with typically smooth surfaces. The ceramic head materials include Biolox® Delta (CeramTec North American Corp., Laurens, SC), a mixture between alumina and zirconia, Biolox® Forte (CeramTec North American Corp., Laurens, SC), pure alumina, and pure zirconia.

Sample	Stem Material	Head Materia	Time in Situ (months)	Reason for Revision	Bearing Surface	Taper Score	Sleeve (Y/N)	Original Head/Stem
S1	CoCr	Zirconia	176.2	Infection	C-O-P	1	N	Y
S2	TMZF	Biolox Forte	20.3	Infection	C-O-C	1	N	Y
S3	CoCr	Biolox Forte	154.1	Aseptic loosening	C-O-P	1	N	Y
S4	TMZF	Biolox Forte	14.2	Infection	C-O-C	3	N	Y
S5	CoCr	Biolox Delta	15.4	Aseptic loosening	C-O-P	1	N	Y
S6	CoCr	Biolox Delta	15.6	ALTR	C-O-P	4	Y	Y
S7	CoCr	Biolox Delta	16	ALTR	C-O-P	4	N	
S8	CoCr	Biolox Delta	20.7	ALTR	C-O-P	4	N	
S9	CoCr	Biolox Delta	12.4	ALTR	C-O-P	1	N	
S10	CoCr	Biolox Delta	14.6	ALTR	C-O-P	4	N	
S11	TiAlV	Biolox Delta	25.7	Femoral Loosening	C-O-C	1	N	Y
S12	TiAlV	Biolox Delta	26.6	Femoral Loosening	C-O-C	1	N	Y
S13	CoCr	Biolox Forte	6.0	ALTR	C-O-M	2	Y	N
S14	TMZF	Biolox Delta	38.4	Infection/Loosening	C-O-P	3	N	Y
S15	TiAlV	Biolox Delta	35.9	Infection	C-O-P	2	N	Y
S16	TiAlV	Biolox Delta	19.1	Infection	C-O-P	1	N	Y
S17	TiAlV	Biolox Delta	12.3	Infection	C-O-P	1	N	Y
S18	no stem rec'd, sleeve only	Biolox Forte	7.2	Infection	C-O-P	no stem	Y	N
S19	unidentifie	Biolox Delta	33.3	Infection	C-O-P	1	N	Y
S20	TiAlV	Biolox Delta	15.9	Femoral Loosening	C-O-P	1	N	Y
S21	TiAlNb	Biolox Delta	18.8	Femoral Loosening	N/A	1	N	Y
S22	CoCr	Biolox Delta	87.3	Femoral Loosening	C-O-P	4	Y	N
S23	CoCr	Biolox Delta	26.9	Pain	C-O-P	1	N	Y
S24	TiAlV	Biolox Delta	32.6	Femoral Loosening	C-O-P	1	N	Y
S25	TiAlV	Biolox Delta	24.4	Femoral Loosening	C-O-P	1	N	Y

Table 2: Retrieved Implant Data

Based on the images from the RedLux, several stem tapers were chosen and viewed under the scanning electron microscope. This allowed for high resolution imaging of the tapers to determine corrosion, material transfer, and deformation. The stem tapers studied with the SEM were those that showed areas of damage and unusual topography. Along with the damaged tapers, 3 stem tapers with a damage score of 1 were imaged to demonstrate the original machining lines prior to potential damage. Each of these 3 tapers had a different average machining peak height. The roughest taper had an average height of 13.73 μm, the middle taper had an average height of 6.46 μm, and the smoothest taper had an average height of 1.03 μm. Images were taken at various magnifications ranging from 50X to 4000X to show an overview as well as a closer look at the machining lines and damage areas. From the produced images, type of damage was indicated along with the location of the damage. The damage modes were then correlated to the taper material to determine if there was a pattern.

4 RESULTS

4.1 Aim 1

4.1.1 Ceramic vs. Metal Impaction Force

Of the 32 surgeons tested in round 1 of data collection, 15 returned for the second round of testing. The 4 medical students tested had already left for their next specialty rotation, so they will not be included in the data analysis. The remaining 13 surgeons that did not return failed to respond to inquiries of scheduling a time for the second round of data collection. This resulted in 7 attendings, 2 fellows, and 6 residents for comparison analysis. The surgeon connected to subject identifier HT_24 stated that they perform half of the hip replacement surgeries with the right hand, and the other half with the left hand. Therefore, this subject was tested using both hands. The results directly comparing metal and ceramic head impaction force for these 15 surgeons are illustrated below in Figure 8.

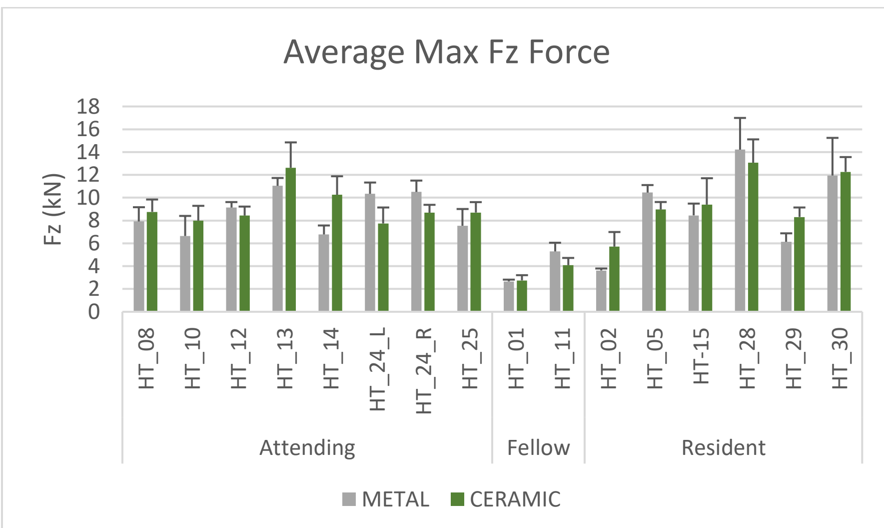

Figure 8: Average maximum Fz force comparing metal and ceramic femoral heads

Looking at the data from these 15 surgeons, the direct comparison shows that 10 of them used a greater impaction force when hitting the ceramic head, while the remaining 6 used a greater force on the metal head. Subject HT_24, who was tested with both hands, had a consistently greater impaction force on the metal head ($p=0.012$; $p=0.01$) using the left and right hands. The metal impaction force was 10.34 kN for the left hand, and 10.50 kN for the right hand. The ceramic head impaction force measured 7.74 kN using the left hand, and 8.69 kN using the right hand. Statistical data reporting the p-values for each surgeon's impaction force and angle can be found in Appendix C and Appendix D. Through statistical analysis, 7 of the 16 direct comparisons of metal vs ceramic impaction force in the Z direction showed a significant difference ($p<0.05$). One attending (right and left-handed impaction), one fellow, and one resident hit the metal head significantly harder than the ceramic head. Meanwhile, two residents and one attending impacted the ceramic head with a significantly greater force than the metal.

An overview of the applied forces for the metal heads as compared to the ceramic heads for all 28 surgeons is shown below in Table 3. According to the data, attendings and residents used a greater impaction force on the metal heads. On average, attending surgeons applied a force of 8.74 kN to the metal heads along the Z-axis. This is compared with an average of 8.72 kN that was applied the ceramic heads, which is not a significant difference ($p=0.982$). There are similar results for the residents in that the impaction force applied to the metal head was greater, but not by a significant value ($p=0.839$). The fellows impacted the ceramic head with a larger force at 6.99 kN than the metal head at 5.03 kN ($p=0.474$). This average maximum Fz force data is represented graphically in Figure 9.

Average Maximum Fz Force (kN)

Surgeon Level	Metal Head	Ceramic Head
Attending	8.74	8.72
Fellow	5.03	6.99
Resident	8.97	8.69

Table 3: Average maximum Fz force comparing metal and ceramic femoral heads

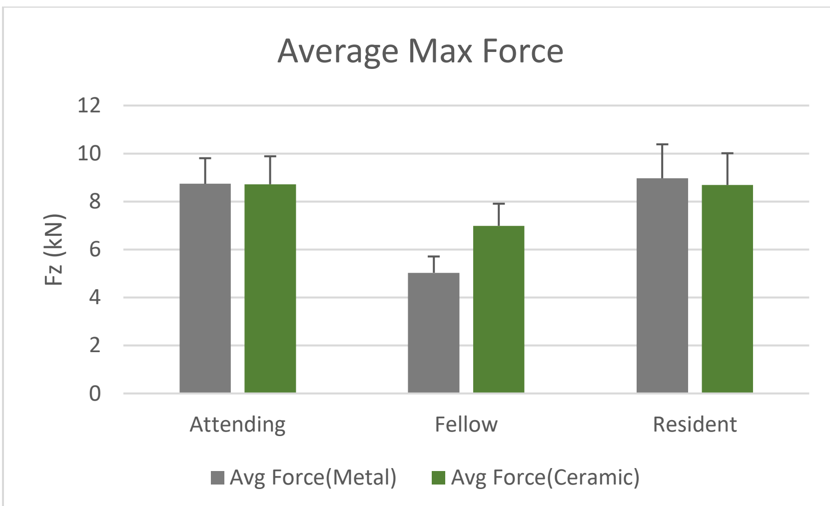

Figure 9: Graphical representation of the average maximum Fz force comparing metal and ceramic femoral heads

4.1.2 <u>Ceramic vs. Metal Angle</u>

For each surgical impaction force measured, the off-axis angle was calculated to determine if there is a difference between metal and ceramic heads. The impaction angle, θz, is illustrated in Figure 7b with the average results summarized below in Table 4. For attendings, the average metal head off-axis angle was 3.7° compared to an average of 5.7° for the ceramic head ($p=0.039$). A lower metal head impaction angle is also seen for the fellows (5.7°) and residents (4.6°). The ceramic head off-axis impaction angle was greater for all surgeon levels with fellows at 8.5°, and residents impacting at an angle of 5.8°.

Average Off-Axis Impaction Angle, θz (degrees)

Surgeon Level	Metal Head	Ceramic Head
Attending	3.7 (1.4)	5.7 (2.2)
Fellow	5.7 (2.3)	8.5 (2.2)
Resident	4.6 (2.5)	5.8 (1.2)

Table 4: Average off-axis impaction angle and standard deviation comparing metal and ceramic femoral heads

The diagram in Figure 10 illustrates the location at which the femoral head was impacted by each surgeon. To plot these location graphs, the average maximum Fz data was found along with the corresponding Fx and Fy data. Using MatLab, the x and y data points were converted from cartesian to polar coordinates, which gives the angle and distance from the center. These polar coordinates were then plotted on the location graphs. The MatLab code to produce these graphs can be found in Appendix G. The left side shows the location for the metal head while the right side shows the location for the ceramic head. Each surgeon level is indicated using a different color. It can be seen that the impaction location of the metal head is much more centralized than the location for the ceramic head.

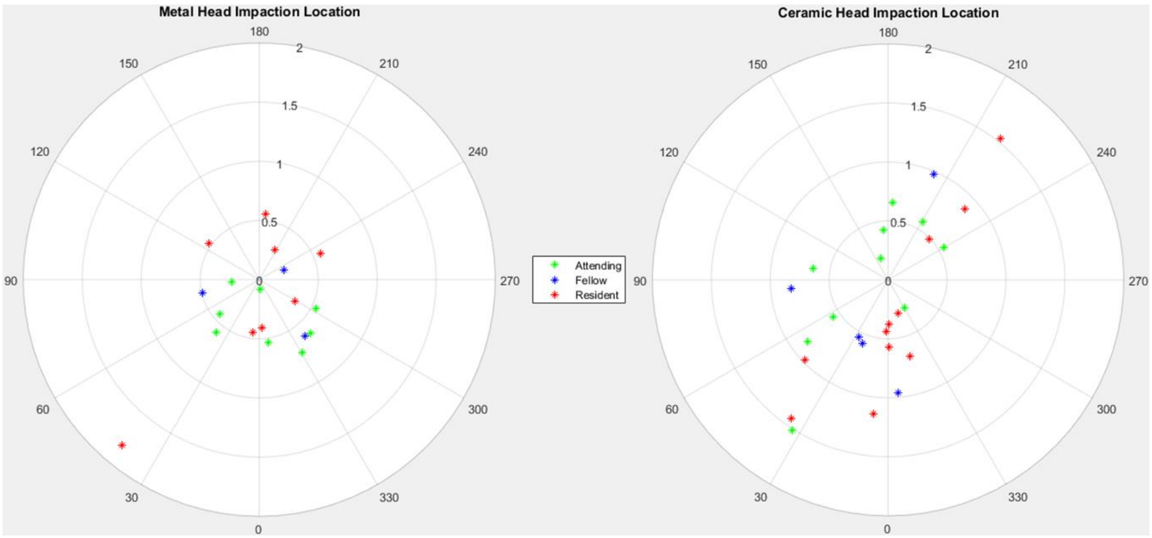

Figure 10: Femoral head impaction location comparing metal and ceramic

4.1.3 Surgeon Experience Level

In addition to comparing metal and ceramic femoral heads, impaction force and off-axis angle were assessed based on surgeon experience level. Attending surgeons and residents had similar impaction forces. Attendings impacted the ceramic heads with a larger force than the residents (p=0.973), but the residents impacted the metal heads with a larger force than the attendings (p=0.868). However, the difference in these forces was not significant. Combining metal and ceramic, fellows had the lowest impaction force in the Fz direction, when compared with attendings (p=0.265) and residents(p=0.331), but not by a significant value. These comparisons are also graphically represented in Figure 9.

To determine variability within surgeon experience levels, the standard deviation of each level was calculated and is displayed Table 5.

Standard Deviation Across Surgeon Levels

Surgeon Level	Metal Head	Ceramic Head
Attending	1.8	1.7
Fellow	2.3	3.9
Resident	3.4	2.6

Table 5: Standard deviation across surgeons of the same level

For both metal and ceramic femoral heads, attending surgeons had the smallest standard deviation of 1.8 for metal and 1.7 for ceramic, indicating the lowest variability among surgeons. This was followed by fellows at 2.3, and then residents at 3.4 for metal heads. Ceramic heads had residents at the second lowest standard deviation of 2.6 and fellows at 3.9 (Figure 11, Figure 12). Although a resident had the greatest individual impaction force for each material, the averages show almost the same force between attendings and residents.

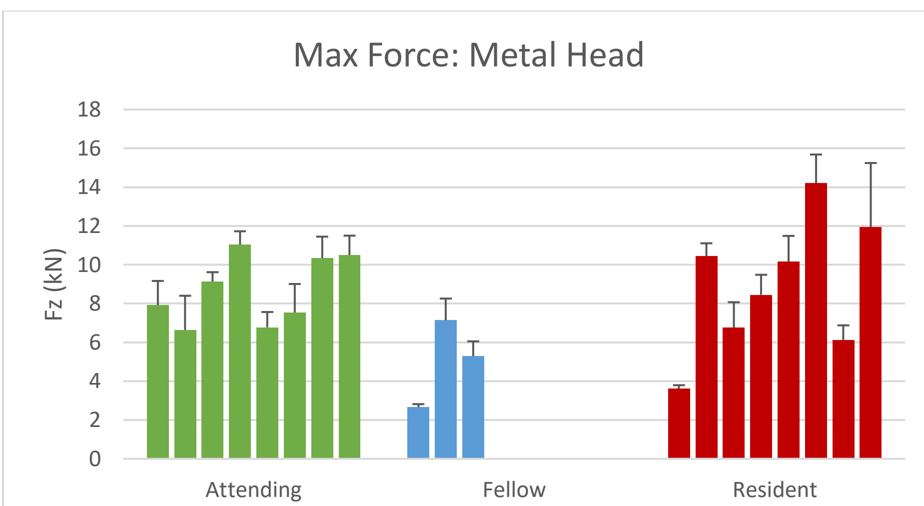

Figure 11: Average maximum metal head impaction force, Fz, for each surgeon

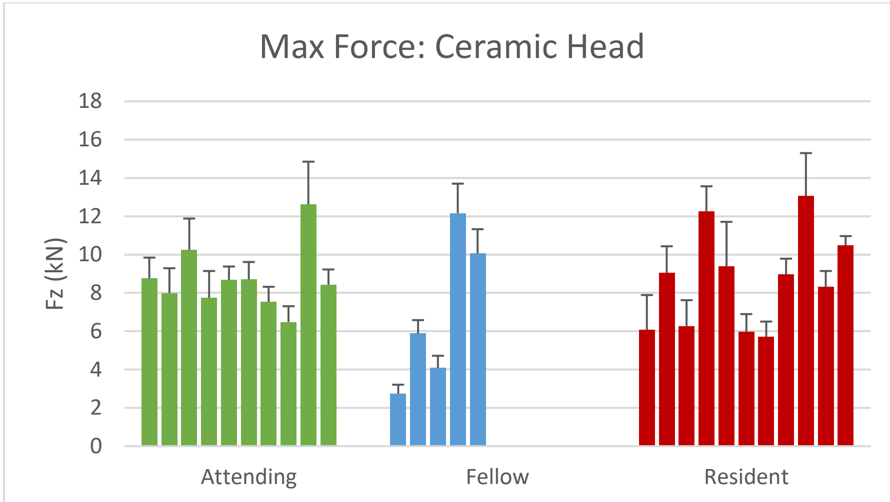

Figure 12: Average maximum ceramic head impaction force, Fz, for each surgeon

Overall forces and angles combining metal and ceramic are shown below in Figure 13. These visually display that attending surgeons had the smallest range of values for impaction force, Fz. Fellows had the lowest impaction force in the Z direction, when compared with attendings ($p=0.265$) and residents($p=0.331$), but not by a significant value. With respect to the impaction angle, θz, and the data shown in Table 4, overall, attendings ($p=0.010$) and residents ($p=0.017$) had a significantly lower impaction angle than fellows. Attendings and fellows had a similar span of data, but the fellows' off-axis angle was much higher than the attendings'.

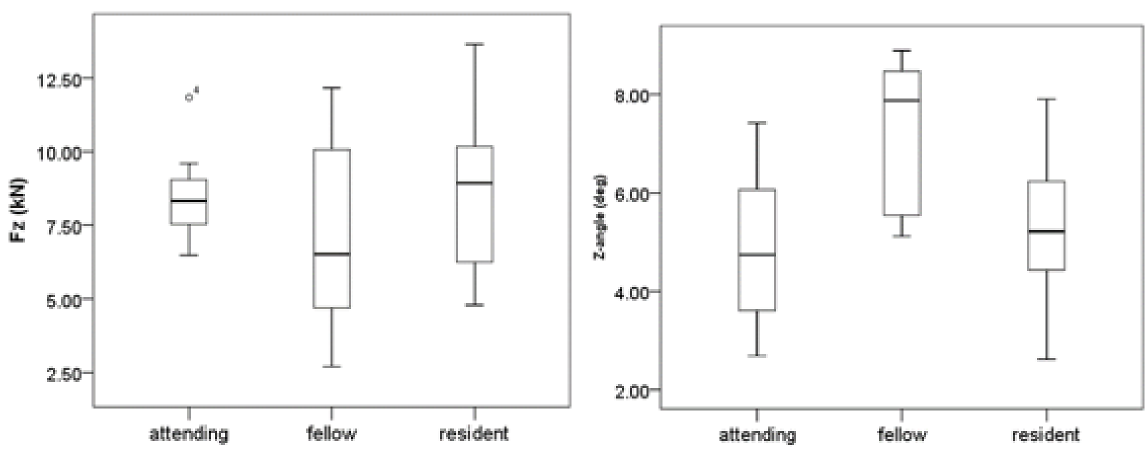

Figure 13: Box plots representing overall values per surgeon experience level

The collected responses to the surgeon exit questionnaire are displayed below in Table 6. The mode response to each question is recorded in the last row. Every surgeon that completed the questionnaire believes that both the impaction force and number of strikes can affect the success of the hip implant. Also, 93% of the surgeons think that a metal femoral head has greater fracture resistance. Of the 15 responses, 80% (12 surgeons) recorded that they apply the same amount of force to the ceramic head as they do the metal head. However, the data shows that only 7 of these 12 surgeons actually did apply the same force to both materials. Another 2 surgeons indicated that they do not apply the same force to metal and ceramic, but actually did. While 13% (2 surgeons) report hitting metal harder than ceramic, neither of these surgeons actually impacted metal harder. An additional 3 other surgeons hit the metal head harder than the ceramic head, although stating otherwise in the questionnaire.

	1=Yes; 2=No; 3=Somewhat	1=Posterior; 2=Anterior; 3=Anterolateral; 4=Direct Lateral; 5=Other	1=Yes; 2=No	1=Yes; 2=No	1=Always; 2=Sometimes; 3=Rarely; 4=Never	1=Always; 2=Sometimes; 3=Rarely; 4=Never	1=Metal; 2=Ceramic; 3=They're Equal	1=More Force; 2=Less Force; 3=Same Force
Sub ID#	**Q1**	**Q2**	**Q3**	**Q4**	**Q5**	**Q6**	**Q7**	**Q8**
HT-01	1	1	1	1	1	3	1	2
HT-02	1	1	1	1	2	2	1	3
HT-05	3	1	1	1	2	2	1	3
HT-08	3	1	1	1	1	2	1	3
HT-10	3	1	1	1	1	2	1	3
HT-11	2	1	1	1	4	3	1	3
HT-12	3	1	1	1	2	2	1	3
HT-13	3	2	1	1	1	3	1	3
HT-14	3	1	1	1	1	3	1	3
HT-15	1	1	1	1	1	2	1	3
HT-24	1	1	1	1	1	1	3	3
HT-25	1	1	1	1	1	2	1	3
HT-28	3	1	1	1	1	3	1	3
HT-29	3	1	1	1	2	2	1	2
HT-30	1	1	1	1	1	2	1	1
MODE	**3**	**1**	**1**	**1**	**1**	**2**	**1**	**3**

Table 6: Surgeon exit questionnaire responses

4.1.4 Impulse

For each surgical impaction, a graph showing the peak data was created. An example of this is shown below in Figure 14. Each graph is a zoomed in look at each of the strikes applied during femoral head assembly. The graph from the first strikes shows more vibrations than strikes two or three. These vibrations are residuals forces that occurred as the femoral head settled onto the stem taper. The potential impact of multiple strikes on the implant needs to be further investigated.

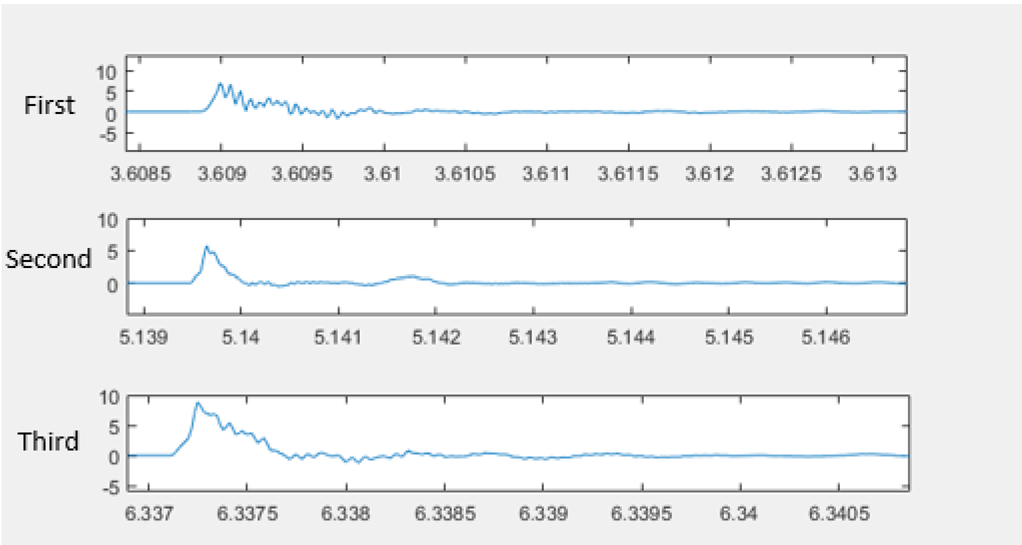

Figure 14: Peak impaction force graphs for each strike applied during assembly

4.2 Aim 2

4.2.1 Stem Taper Scores

For each of the 25 retrieved implants, the stem taper was scored using the Goldberg method. This gives each taper a score from 1-4 based on the amount and level of corrosion. A total of 15 stems included in this study received a taper score of 1, correlating to no visible corrosion. Two stem tapers had a score of 2, indicating mild corrosion. Two tapers were given a score of 3 for moderate corrosion. The remaining 5 tapers were scored a 4, representing severe corrosion. One of the retrieved implants did not have a stem included; there was only a sleeve. The taper scores correlating to each implant are shown in Table 7.

Sample	Taper Score
S1	1
S2	1
S3	1
S4	3
S5	1
S6	4
S7	4
S8	4
S9	1
S10	4
S11	1
S12	1
S13	2
S14	3
S15	2
S16	1
S17	1
S18	no stem
S19	1
S20	1
S21	1
S22	4
S23	1
S24	1
S25	1

Table 7: Retrieved implant taper scores

4.2.2 Metrology Optical Coordinate Measuring Machine

The RedLux profiler produces images of the stem and head taper surface topography which includes a height scale to help visualize the variances in surface height. The image in Figure 15 shows the overall stem taper topography of CoCrMo with evidence of scratches indicated by the arrow. As shown in the corresponding height reference, the dark coloration of the scratches designates a lower height on the taper surface. This damage could have occurred during removal of the head of the hip implant.

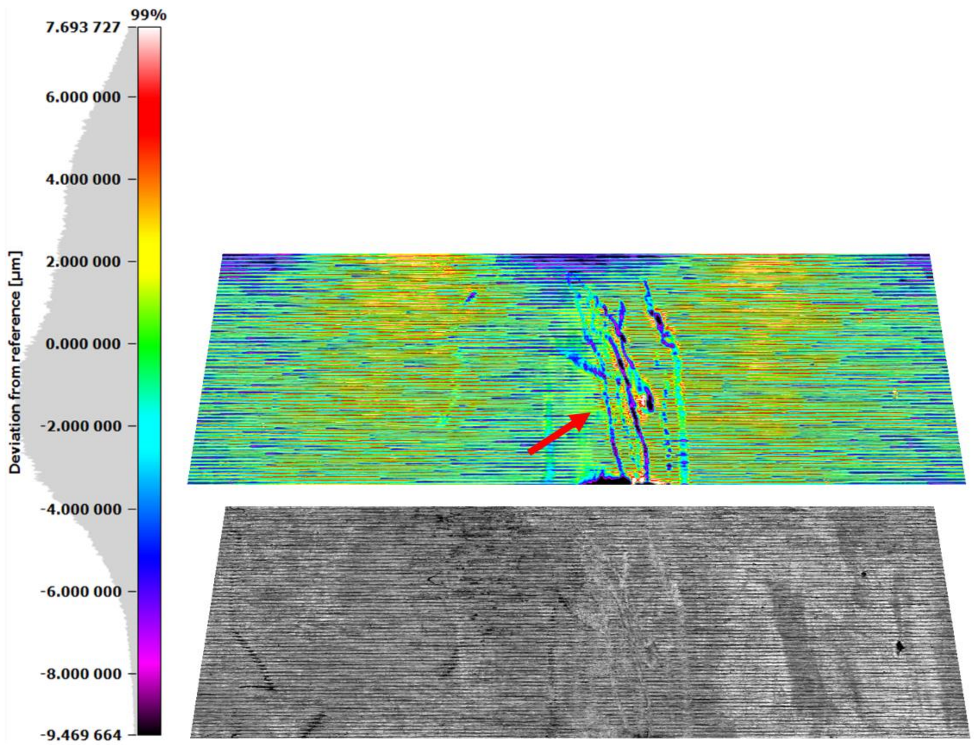

Figure 15: CoCrMo stem taper, S23, with surgeon damage

Images taken of the head tapers can show areas of material transfer from the stem to the femoral head interior. One of these cases is illustrated below in Figure 16 where the light color on the scan, denoted by the arrow, indicates a higher surface of approximately 4.78 µm. This is probably material transfer from the TiAlV stem taper. The corresponding dark spot on the sensor scan below shows an area of irregular surface compared to the machined topography.

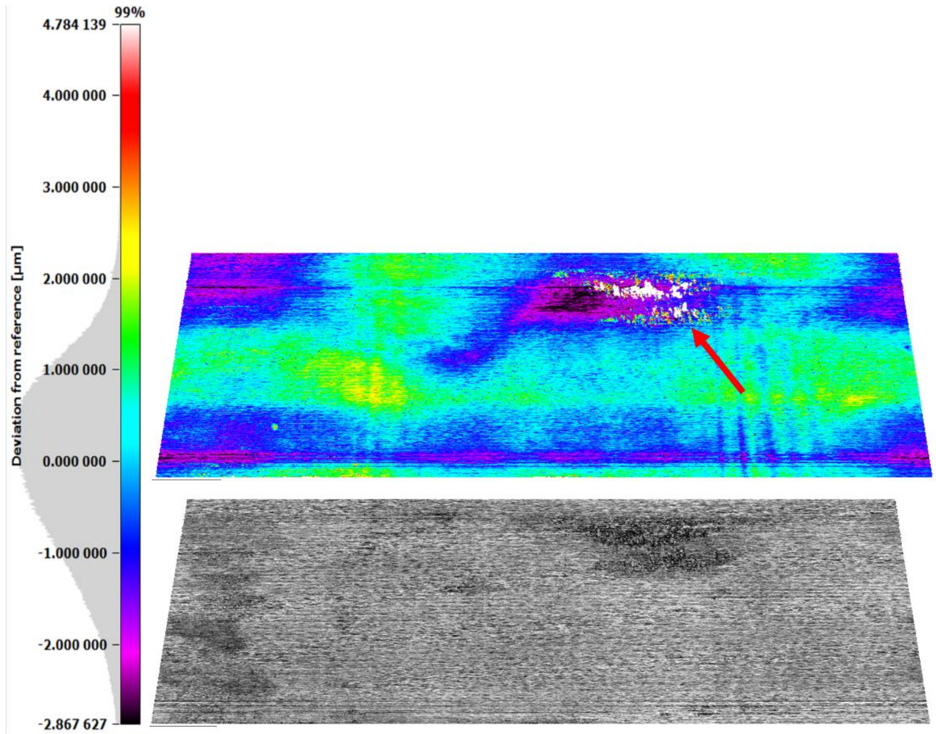

Figure 16: Head taper of TiAlV stem, S15, showing material transfer

A head taper with a corresponding CoCrMo stem taper also illustrated areas of material transfer (Figure 17). Again, the light-colored spots on the topography height image indicate a raised surface relative to the machined surface. These areas are at about 4.17 µm in height. The grayscale sensor scan shows darkened areas, corresponding to the material transfer.

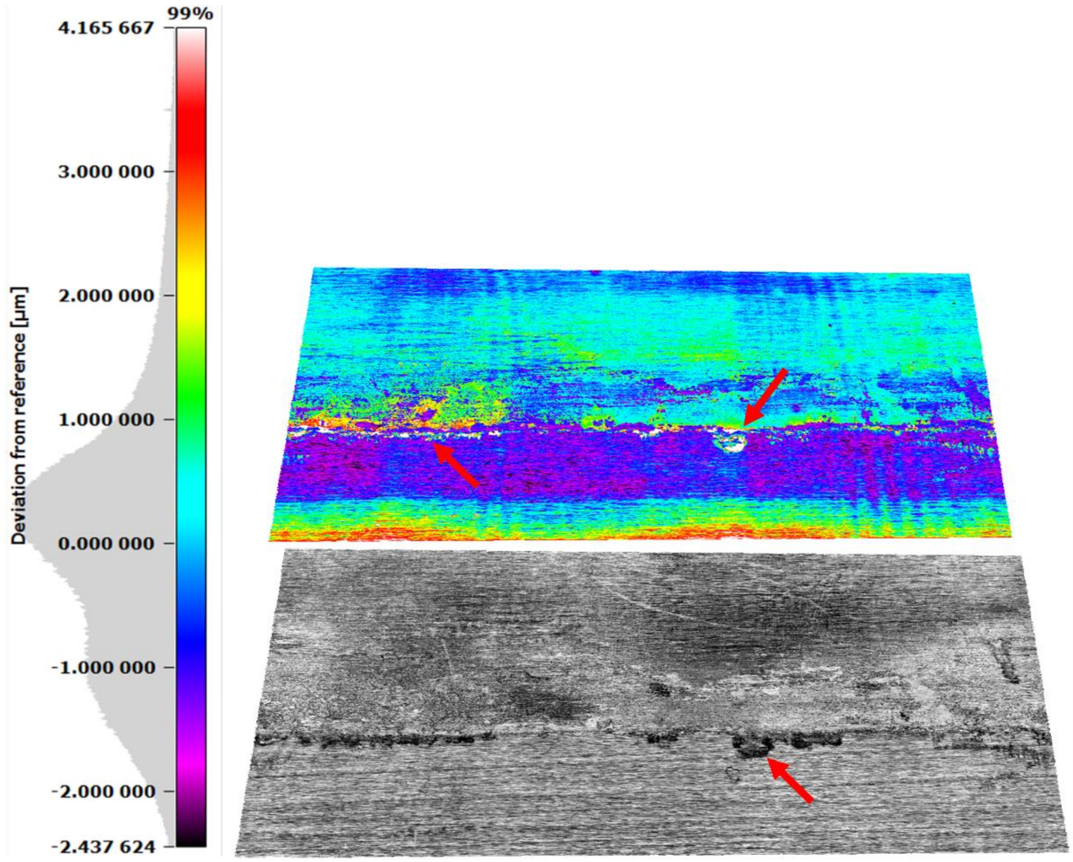

Figure 17: Head taper of CoCrMo stem, S7, with evidence of material transfer

4.2.3 Scanning Electron Microscopy

The scanning electron microscope (SEM) was used to further investigate areas of corrosion or damage from the surgery. The RedLux images previously shown provided a guide as to which stem tapers had the most extensive damage, and at what locations. The SEM image shown below in Figure 18 is of a TMZF alloy stem taper at 500X magnification. The arrows indicate locations of plastic deformation where contact with the femoral head likely occurred. The cuts and grooves on the surface most probably happened during the machining process.

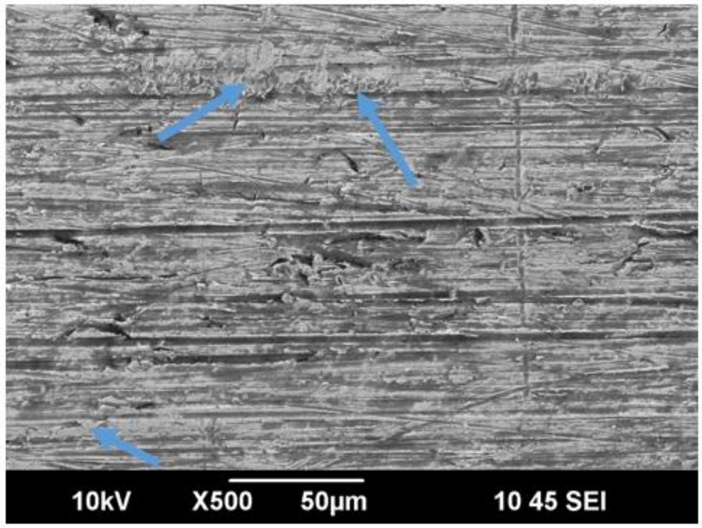

Figure 18: TMZF alloy, S2, indicating machining marks and deformation

The image at 500X magnification of a CoCrMo stem taper (Figure 19) shows areas of flattening of the machining mark peaks, indicated by the arrows. This damage likely happened when the surgeon was assembling the femoral head or disassembling the femoral head.

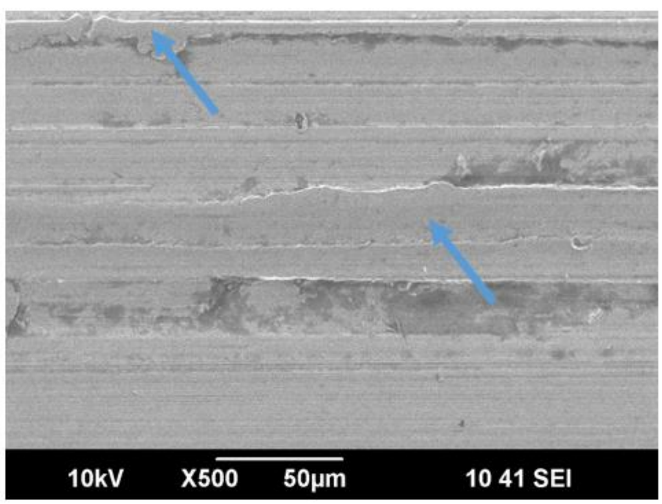

Figure 19: CoCrMo stem taper, S3, with machining peak deformation

A similar case of another CoCrMo stem taper with evidence of deformation of the machining mark peaks is shown below in Figure 20. The magnification of 4000X allows for a closer, more detailed look of the vertical marks on the machining lines, indicating that this deformation most probably occurred during assembly or disassembly of the implant.

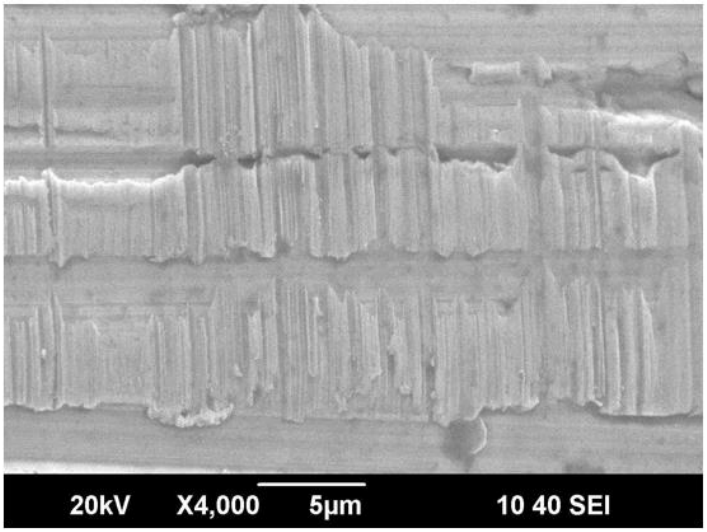

Figure 20: CoCrMo taper, S9, with peak flattening from assembly/disassembly

The stem taper below in Figure 21 is made of a powder metallurgical CoCrMo alloy, in which metal powder was sintered to form the stem taper. The image on the left shows evidence of fretting corrosion. The arrows in the image on the right point to areas of pitting corrosion that occurred in the troughs of the topography. This stem was paired with a metal sleeve; however, the ceramic head was the original femoral head for this hip implant.

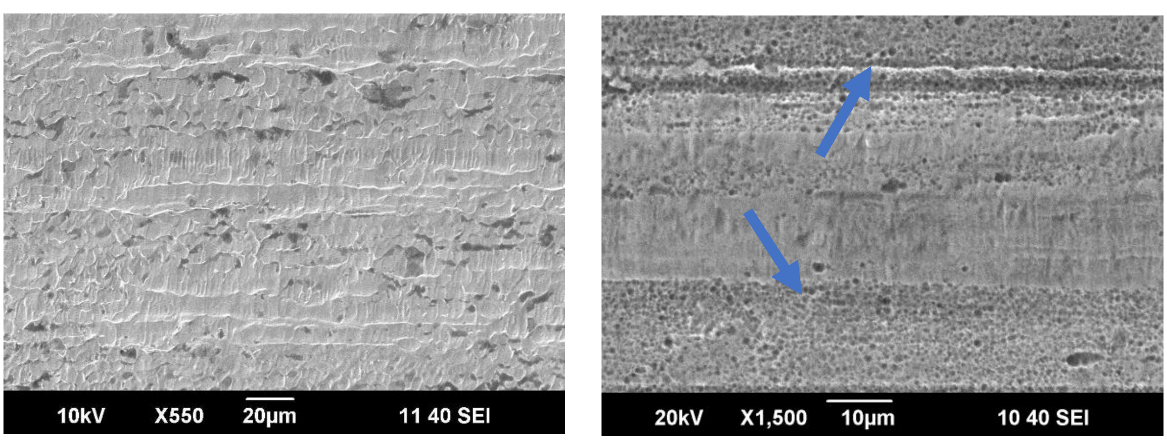

Figure 21: Fretting and pitting corrosion on a CoCrMo stem taper, S6

A CoCrMo cast alloy stem taper (Figure 22) was scanned at 100X and 500X magnification. The lower magnification image on the left shows intergranular corrosion evidenced by the cracking appearance of the surface. The 500X image on the right shows a case in which entire grains fell out due to the intergranular corrosion.

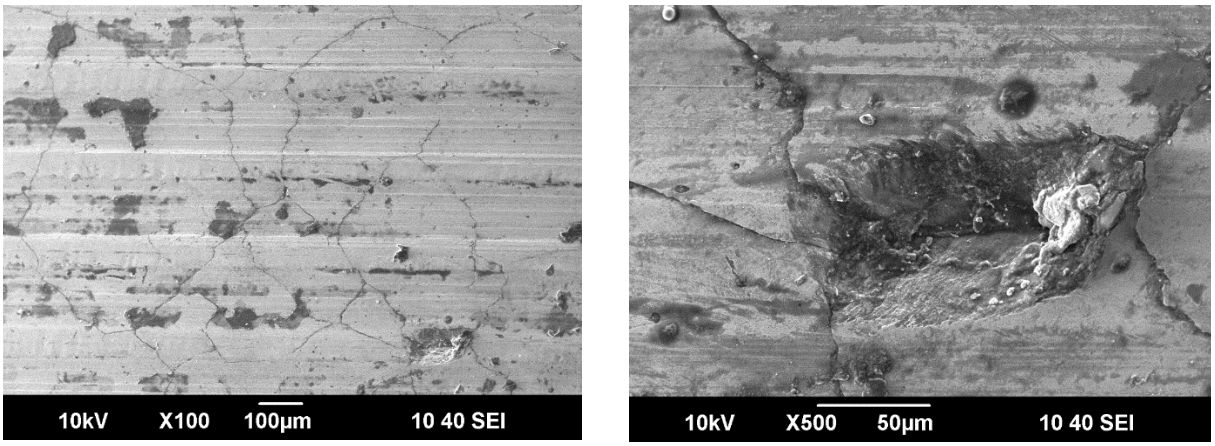

Figure 22: CoCrMo stem taper, S22, with intergranular corrosion

This final case is a TMZF alloy stem taper (Figure 23). The blue arrow indicates an area of organic matter on the surface, and the red arrows indicate layers of compacted wear debris. The right side is a back-scatter image that detects the atomic number of the different areas. The dark color indicates a lower atomic number confirming there is organic material. The wear debris layers consist of Ti-oxide, leading to a darker area.

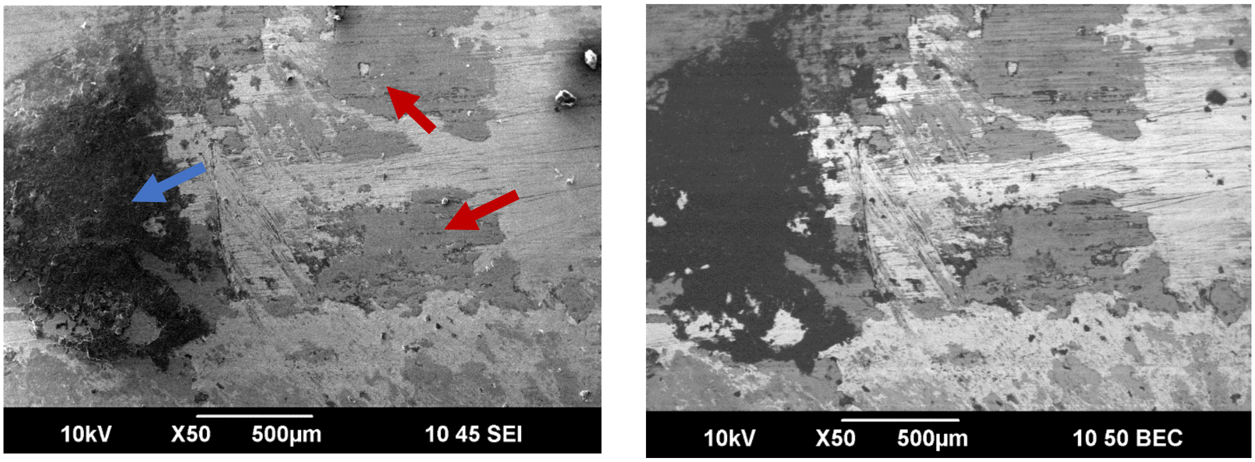

Figure 23: TMZF alloy. S14, with organic matter and wear debris

4.2.4 Zygo Surface Profiler

Each retrieved stem taper and head taper was viewed and measured using the Zygo 3D Surface Profiler. The profiles taken were areas of little wear on the surface, in order to view the original topography. The surface topography profiles collected were then analyzed in MatLab where the average machining mark heights and spaces were calculated. The data collected for each stem taper and head taper is summarized in Table 8. The head tapers all had fairly smooth surfaces, with the largest height being 2.5 µm. However, the stem tapers had varying roughness ranging from 0.78 µm to 13.9 µm. The material with the smallest stem taper height, or smoothest topography, was the TMZF. All of the TiAlV stem tapers had rough surfaces with the average machining height of approximately 12 µm. The CoCrMo stem tapers had varying roughness with some having smooth surfaces and some having a rougher topography.

Zygo Stem Taper Data		
	Avg Height(µm)	Avg Spacing(µm)
PT05-301	7.7918	186.0571
PT06-031	1.0312	57.2967
PT06-122	6.4559	199.4286
PT08-025	1.0823	100.72
PT10-285	13.7311	204.0909
PT12-046	2.3044	54.9167
PT12-046 (sleeve)	12.6774	201.3636
PT12-089	0.88729	38.3243
PT12-111	1.0684	48.0625
PT12-113	0.78429	51.9184
PT12-116	1.241	54.1122
PT13-301	12.3991	200.7917
PT13-323	10.9193	199.6522
PT13-352	13.9423	174.0769
PT13-352 (sleeve)	3.2947	124.8
PT14-176	0.80409	43.8444
PT15-074	12.3923	204.3182
PT15-109	12.2654	196.5833
PT15-190	13.4817	203.9545
PT17-062 (sleeve)	1.8972	65.16
PT17-215	12.5511	200.7826
PT17-319	8.3707	206.5455
PT17-319 (sleeve)	11.7156	249.8889
PT18-008	8.6936	205.0455
PT18-031		
PT18-069	11.1096	205.4091

Zygo Head Taper Data		
	Avg Height(µm)	Avg Spacing(µm)
PT05-301	2.2966	94.8158
PT06-031	2.5349	101
PT06-122		
PT08-025	1.6649	106.6056
PT10-285	1.2786	91.2532
PT12-046	2.299	76.0526
PT12-089	1.2576	66.7922
PT12-111	1.0659	68.5664
PT12-113	1.3663	70.7706
PT12-116	0.96143	68.0921
PT13-301	1.4238	72.0741
PT13-323	1.4678	79.0421
PT13-352	0.98674	74.2615
PT13-352 (sleeve)	1.3224	75.7273
PT14-176	1.0835	72.3188
PT15-074	1.152	82.402
PT15-109	1.4865	83.7627
PT15-190	1.4786	84.6897
PT17-062 (sleeve)	1.9589	76.0333
PT17-214	1.0637	73.5347
PT17-215	1.1669	88.1744
PT17-277	1.434	105.2381
PT17-319	2.5212	77.4848
PT17-319 (sleeve)	2.6253	68.0667
PT18-008	1.1321	49.5566
PT18-031	1.4023	67.5304
PT18-069	1.19	61.5357

Table 8: Average machining mark height and spacing of retrieved stem and head tapers

The 3D and 2D surface profiles of a TiAlV stem taper are shown in Figure 24. For this taper, the surface was fairly rough with an average machining mark height of 13.48 µm. The paired head taper had an average height of 1.48 µm.

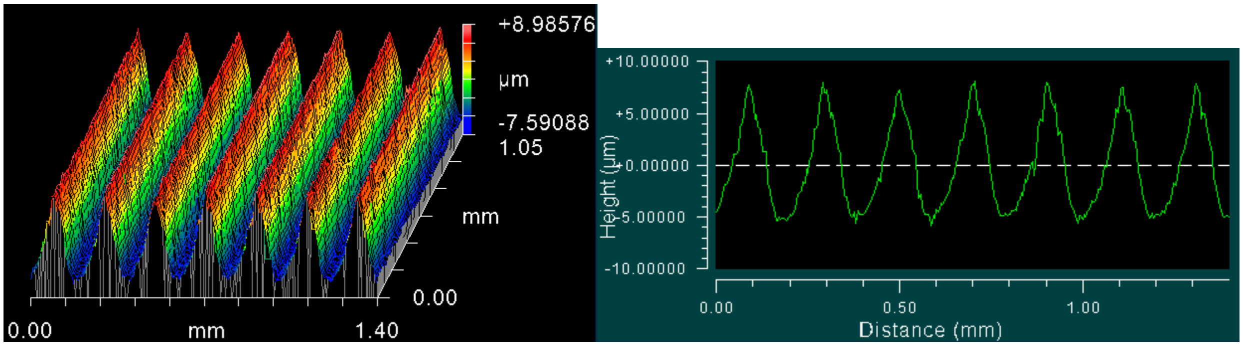

Figure 24: Surface profile of TiAlV stem taper, S17

A CoCrMo stem taper with surface roughness of 6.46 µm has the surface profiles displayed in Figure 25. Of the CoCrMo stems, this one has a surface roughness in the middle range, as some of the tapers are smooth and some are very rough.

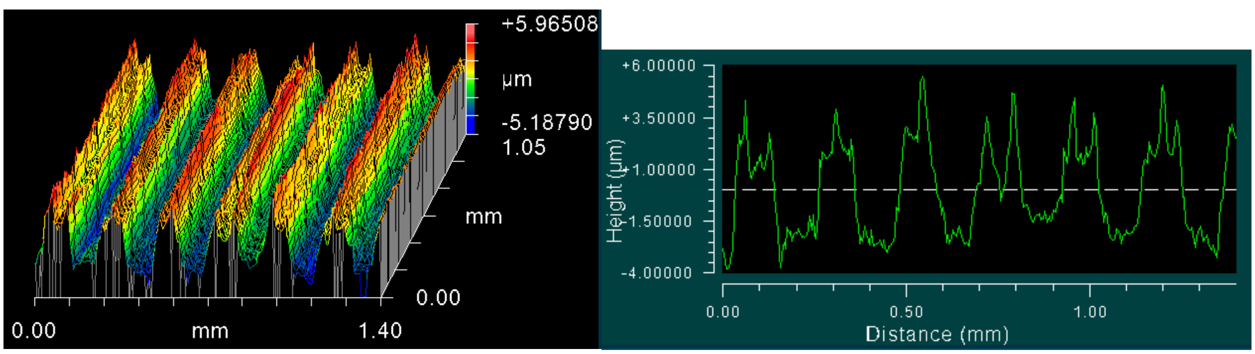

Figure 25: Surface profile of CoCrMo stem taper, S3

The final surface profile image below shows a TMZF alloy stem taper (Figure 26). These tapers are characteristically smooth with very low machining mark heights. The average height for this taper was measured at 1.08 µm.

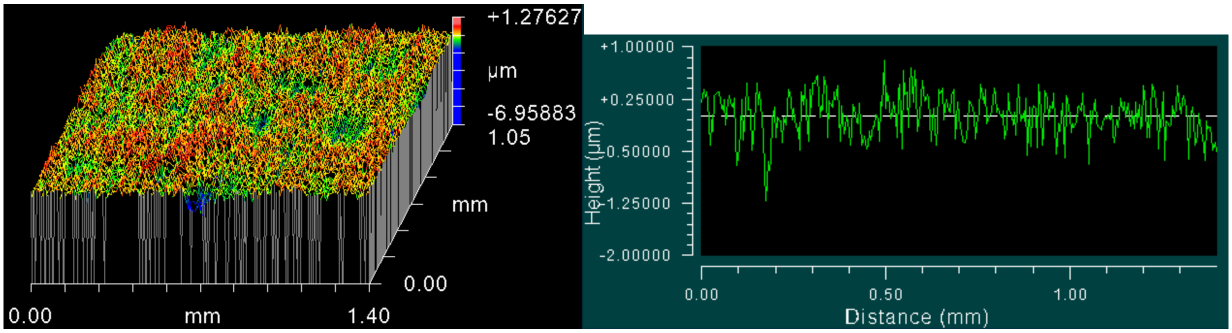

Figure 26: Surface profile of TMZF alloy stem taper, S4

5 DISCUSSION

5.1 Aim 1

The hypothesis that surgeons would impact the metal head with a greater force than the ceramic head was rejected on a group level, however some individuals exhibited significant differences depending on head material. One attending, one fellow, and one resident hit the metal head significantly harder, while one attending and two residents hit the ceramic head significantly harder. Overall, attendings and residents used a greater force on metal femoral heads, but not by a significant value. On average, fellows impacted the ceramic head with a greater force. However, this is due to the fact that a total of 4 fellows impacted the ceramic head, and only 2 impacted the metal head throughout the duration of the study. A direct comparison between the two fellows that impacted both metal and ceramic, shows a greater impaction force on the metal head. Previous studies indicated that the ideal impaction force is 4 kN. This was determined by having surgeons impact a film and then the implant was assembled with a drop hammer based on the force data received (Heiney et al., 2009). Studies such as this do not replicate a hip replacement surgery to determine loads. The surgeons in this thesis study applied forces much greater than 4 kN to both metal and ceramic heads. For attendings and residents, the forces were close to 9 kN. For fellows, the forces were between 5 kN and 7 kN. This shows that the surgeons involved in the study from Rush University Medical Center are more aware of the corrosion possibilities with a small impaction force.

With respect to surgeon experience level, attendings and residents had the greatest impaction force and lowest off-axis angle. It appears that surgeons operating or receiving training at an institution such as Rush University Medical Center are more aware of the problems with taper corrosion, and therefore apply larger, more accurate assembly loads. However, this was a small study conducted at only one institution. Smaller hospitals without a research division may not be aware of the potential impacts of a small assembly load. This could increase the incidence of taper corrosion and implant loosening. To better understand assembly technique and force applied, it is important to expand this research to incorporate other universities and teaching hospitals.

Off-axis forces in both the X and Y directions indicate that there was not a significant difference in the force values of different surgeon experience levels. However, for all levels, the impactions on the metal femoral head were more accurate on the center of the head than the ceramic head. The larger size of the metal head may have contributed to this result. There was no significant difference in the off-axis forces applied to metal and ceramic femoral heads. However, the average forces in the X-direction ranged from 0.5 kN to 4.1 kN and was greatest for residents. The forces in the Y-direction were not as large but ranged from 0.4 kN to 2.5 kN. These off-axis forces can contribute to inadequate seating of the head and increase the risk of component loosening. During “settle in” from the first impaction strike of the femoral head, more residuals forces could be seen on the peak force graph. These forces could be indicative that the first strike is the most crucial for head stability. It could also indicate that additional strikes are needed to create a strong bond between the head and stem taper. Further research into the effect of the impulse is needed.

Utilizing feedback from the surgeons, future iterations of this study could benefit from a testing setup that can be placed at any orientation to accommodate the varying surgical techniques. Also allowing the surgeons to choose the hammer used for impaction would alleviate some of the concerns related to the accuracy of the setup. Other improvements may include using a cadaver instead of a benchtop assembly and also incorporating a force sensor inside the impactor. This will allow an analysis of forces into the system compared to forces out of the system.

This study, along with future studies, could potentially be used as a teaching tool for hip implant assembly. While 14 of the 15 surgeons stated in the surgeon questionnaire that they use a posterior approach, the observations and comments received suggest a wide variance in assembly technique. Also, the data indicates a range of impaction forces used to assemble the femoral head. Expanded testing and results could contribute to surgical education regarding implant assembly technique and the ideal force to prevent corrosion and component loosening.

5.2 Aim 2

Of the 25 retrieved hip implants, 8 of the RedLux scans showed evidence of material transfer on the head taper. With the exception of 3 implants with unknown data, all of these implants were the original stem and femoral head components. This is evidence of a strong bond between the femoral head and stem taper. More research is needed to determine if material transfer is a good thing. This material interaction between the stem and head may contribute to the increased success of ceramic hip implants for active patients.

Many of the head taper RedLux scans had similar patterns of topography that indicate a surface that is not round. The surface height spanned a range of about 6 μm from the areas of a lower surface to the areas of a higher surface. The asymmetrical shape most likely occurred during the manufacturing process of the ceramic head. This unroundness of the femoral head taper will lead to less contact area between the head and the stem, which can then cause less stability of the implant. Another effect is that fluid may be able to enter between the stem and femoral head, leading to corrosion on the stem or sleeve surface.

The surface topography of the stem tapers paired with ceramic heads shows incidences of fretting and intergranular corrosion. One of the reasons surgeons began using ceramic heads was to combat corrosion and increase the life of the implant. The SEM images taken during this study show that different types of corrosion still occur with a ceramic-on-metal interface. However, in many cases, the damage may have originated from a previous metal head, or being paired with a metal sleeve. This connects both aims of this study in that a greater impaction force during assembly can improve the bond between the head and stem. This will lower the risk of micromotion and thereby lessen the frequency of corrosion.

6 CONCLUSION

Although surgeons did not impact the metal head with a greater force than the ceramic head, there was still no evidence of continuity among surgical technique or force applied. This study can help propel further investigation into impaction technique and lead to the development of a guideline on the best assembly approach. This would help train surgeons and also educate them on the adverse effects caused by poor bonding between components that can occur due to insufficient impaction force.

Adverse effects such as corrosion and material loss were identified in this study. While ceramic heads improve implant life and range of motion, there are still cases in which corrosion can occur. A way to help prevent this is to ensure the stem taper is clear of debris. It is also crucial to apply a great enough impaction force to create a strong bond between the stem taper and femoral head. Because ceramics heads recently became more popular than metal heads, more time is needed to determine failure modes that are specific to ceramic heads.

CITED LITERATURE

Cooper, H.J., Jacobs, J.J., Leikin, J.B., Barden, R.M., and Rosenberg, A.G. (2013). Elevated Serum Metal Levels from Vitamin Supplementation: A Case Report. JBJS Case Connect. *3*, e18.

Danoff, J.R., Longaray, J., Rajaravivarma, R., Gopalakrishnan, A., Chen, A.F., and Hozack, W.J. (2018). Impaction Force Influences Taper-Trunnion Stability in Total Hip Arthroplasty. J. Arthroplasty *33*, S270–S274.

D'Antonio, J.A., Capello, W.N., and Naughton, M. (2012). Ceramic Bearings for Total Hip Arthroplasty Have High Survivorship at 10 Years. Clin. Orthop. Relat. Res. *470*, 373.

Di Laura, A., Hothi, H., Henckel, J., Swiatkowska, I., Liow, M.H.L., Kwon, Y.-M., Skinner, J.A., and Hart, A.J. (2017). Retrieval analysis of metal and ceramic femoral heads on a single CoCr stem design. Bone Jt. Res. *6*, 345–350.

English, R., Ashkanfar, A., and Rothwell, G. (2016). The effect of different assembly loads on taper junction fretting wear in total hip replacements. Tribol. Int. *95*, 199–210.

Frisch, N.B., Lynch, J.R., Banglmaier, R.F., and Silverton, C.D. (2016). The Effect of Impact Location on Force Transmission to the Modular Junctions of Dual-Taper Modular Hip Implants. J. Arthroplasty *31*, 2053–2057.

Goldberg, J.R., Gilbert, J.L., Jacobs, J.J., Bauer, T.W., Paprosky, W., and Leurgans, S. (2002). A multicenter retrieval study of the taper interfaces of modular hip prostheses. Clin. Orthop. 149–161.

Hallab, N.J., Messina, C., Skipor, A., and Jacobs, J.J. (2004). Differences in the fretting corrosion of metal–metal and ceramic–metal modular junctions of total hip replacements. J. Orthop. Res. *22*, 250–259.

Haschke, H., Jauch-Matt, S.Y., Sellenschloh, K., Huber, G., and Morlock, M.M. (2016). Assembly force and taper angle difference influence the relative motion at the stem–neck interface of bi-modular hip prostheses. Proc. Inst. Mech. Eng. [H] *230*, 690–699.

Heiney, J.P., Battula, S., Vrabec, G.A., Parikh, A., Blice, R., Schoenfeld, A.J., and Njus, G.O. (2009). Impact magnitudes applied by surgeons and their importance when applying the femoral head onto the Morse taper for total hip arthroplasty. Arch. Orthop. Trauma Surg. *129*, 793–796.

Hothi, H.S., Berber, R., Whittaker, R.K., Blunn, G.W., Skinner, J.A., and Hart, A.J. (2016). The Relationship Between Cobalt/Chromium Ratios and the High Prevalence of Head-Stem Junction Corrosion in Metal-on-Metal Total Hip Arthroplasty. J. Arthroplasty *31*, 1123–1127.

Knight, S.R., Aujla, R., and Biswas, S.P. (2011). Total Hip Arthroplasty – over 100 years of operative history. Orthop. Rev. *3*, 16.

Kocagöz, S.B., Underwood, R.J., Sivan, S., Gilbert, J.L., MacDonald, D.W., Day, J.S., and Kurtz, S.M. (2013). Does taper angle clearance influence fretting and corrosion damage at the head–stem interface? A matched cohort retrieval study. Semin. Arthroplasty *24*, 246–254.

Kurtz, S.M., Kocagöz, S.B., Hanzlik, J.A., Underwood, R.J., Gilbert, J.L., MacDonald, D.W., Lee, G.-C., Mont, M.A., Kraay, M.J., Klein, G.R., et al. (2013). Do Ceramic Femoral Heads Reduce Taper Fretting Corrosion in Hip Arthroplasty? A Retrieval Study. Clin. Orthop. *471*, 3270–3282.

Lehil, M.S., and Bozic, K.J. (2014). Trends in Total Hip Arthroplasty Implant Utilization in the United States. J. Arthroplasty *29*, 1915–1918.

Ma, L., and Rainforth, W.M. (2012). The effect of lubrication on the friction and wear of Biolox®delta. Acta Biomater. *8*, 2348–2359.

Rehmer, A., Bishop, N.E., and Morlock, M.M. (2012). Influence of assembly procedure and material combination on the strength of the taper connection at the head–neck junction of modular hip endoprostheses. Clin. Biomech. *27*, 77–83.

Restrepo, C., Parvizi, J., Kurtz, S.M., Sharkey, P.F., Hozack, W.J., and Rothman, R.H. (2008). The noisy ceramic hip: is component malpositioning the cause? J. Arthroplasty *23*, 643–649.

Tomek, I.M., Currier, J.H., Mayor, M.B., and Van Citters, D.W. (2012). Metal Transfer on a Ceramic Head With a Single Rim Contact. J. Arthroplasty *27*, 324.e1-324.e4.

Uchiyama, K., Inoue, G., Takahira, N., and Takaso, M. (2017). Revision total hip arthroplasty - Salvage procedures using bone allografts in Japan. J. Orthop. Sci. Off. J. Jpn. Orthop. Assoc. *22*, 593–600.

Valet, S., Weisse, B., Kuebler, J., Zimmermann, M., Affolter, C., and Terrasi, G.P. (2014). Are asymmetric metal markings on the cone surface of ceramic femoral heads an indication of entrapped debris? Biomed. Eng. OnLine *13*, 38.

APPENDICES

Appendix A

Number	Level	M/C	Max Fz (kN	Std Dev	θz (deg)	Max Fx (kN)	Std Dev	θx (deg)	Max Fy (kN	Std Dev	θy (deg)	# Hits
HT_01	Fellow	Metal		0.155639091			0.055089586			0.151762828		
			2.6748		5.569101	0.5827		89.9509652	0.7234		95.56888	
			2.471		3.122065	0.5094		90.67376402	0.3802		93.04836	3
			2.6481		4.176689	0.5793		92.49317269	0.4287		93.34882	
			2.8513		6.528773	0.4701		93.38391941	0.4992		95.57685	
		Ceramic	2.6052	0.462706649	11.35798	0.8281	0.126254287	79.98521699	0.3629	0.025316556	84.69677	
			3.1201		8.041126	0.5758		82.83913206	0.4061		86.36098	
			2.0483		12.75844	0.4831		78.88403071	0.3481		83.81688	3
			3.204		12.03377	0.6284		78.94099171	0.3587		85.31456	
			2.7541		12.28746	0.6271		79.18688029	0.3414		84.2336	
HT_02	R3	Metal		0.171870074			0.094559223			0.241827252		
			3.5153		10.13505	0.9219		81.05898134	1.8607		85.26626	
			3.8365		7.176065	0.959		82.88418368	1.5022		90.92316	1
			3.6806		7.007789	1.0459		83.06893058	1.2869		88.97093	
			3.4553		5.125336	0.8176		85.05732974	1.4506		91.35276	
		Ceramic	5.9915	1.280041971	5.257696	0.922	0.496117882	85.00286748	2.0963	0.50612807	91.63049	
			5.2012		7.550831	1.0489		82.79873805	1.4409		87.74109	
			7.4275		2.85173	2.1157		87.35951979	1.9278		91.07638	1
			6.0092		7.756393	1.6602		82.49523997	1.479		88.05156	
			3.9277		2.045873	1.1669		91.98450576	0.7973		90.49713	
HT_04	R5	Metal										
		Ceramic	5.7396	1.813057494	4.225389	1.2395	0.318002731	89.19159425	0.2215	0.208907013	94.14706	
			6.1629		3.474158	1.0187		86.96501409	0.6813		88.31083	
			3.892		7.443213	0.768		92.96751351	0.2373		96.81993	3
			8.9204		6.282277	1.5635		83.96834368	0.5262		88.24975	
			5.6667		2.539226	0.8682		87.46077936	0.2497		89.99495	
HT_05	R4	Metal	9.5473	0.658847431	3.089903	2.0859	0.202184408	90.18996355	1.35	0.180661747	93.08405	
			11.2634		6.594061	2.3067		94.44322484	1.2707		94.86251	
			10.6268		1.425002	2.1647		88.72139463	1.0527		90.62902	5
			10.0699		3.189799	2.3308		91.33174418	0.9708		92.89797	
			10.74		2.829798	1.8304		91.10995375	0.9522		92.6027	
		Ceramic	9.3362	0.661103867	2.893226	1.8143	0.276440223	87.57950113	1.7445	0.564433889	91.58397	
			9.2558		7.169059	1.5595		84.70370246	2.6954		85.18217	
			9.4559		6.921375	1.3923		86.17094195	1.8005		84.24288	3
			8.9231		8.473024	1.962		83.34254116	1.3244		84.78245	
			7.8322		9.552344	1.3098		86.83433768	1.3032		80.99674	
HT_06	R2	Metal	8.4548	1.310417566	3.491428	1.5935	0.478027497	92.67889818	1.1044	0.280387405	92.23747	
			7.7978		3.113508	2.8211		92.7597185	1.2175		91.44037	
			5.34		1.408574	1.8539		91.39026548	0.7684		90.22633	2
			5.9573		0.852584	1.8575		89.43837701	0.8133		89.35855	
			6.2514		4.237528	2.2463		93.95628679	0.5148		91.51562	
		Ceramic										
HT_07	Fellow	Metal										
		Ceramic	5.5953	0.695101869	10.02391	1.1771	0.139777366	93.65478407	1.4731	0.275864817	80.67894	
			5.663		8.501378	1.2691		83.21180045	1.416		84.90604	
			6.9474		8.676	1.3703		87.28004897	1.6559		81.76763	2
			6.1232		7.82772	1.5443		90.99657239	1.7489		82.23677	
			5.1014		9.41419	1.4103		91.83296376	1.035		80.76916	
HT_08	Attending	Metal	6.462	1.245838988	4.309351	0.8685	0.410495959	86.43988847	1.4237	0.534282404	92.42506	
			7.5613		3.617406	1.1613		88.15369707	2.26		93.10968	
			7.6084		9.033011	1.9387		83.57418313	2.5919		96.3218	2
			8.0927		3.176118	1.2626		86.9008275	1.9768		90.6942	
			9.8763		3.527946	1.5805		88.23366457	2.7765		93.05296	
		Ceramic	8.0348	1.084797563	3.146303	2.8707	0.451883589	90.93706061	1.6225	0.105837011	93.00325	
			7.3403		11.775	2.0105		83.54158572	1.5329		80.19647	
			8.8557		3.494016	3.0748		92.33517939	1.806		87.40239	2
			9.5854		9.167351	2.8239		82.29718731	1.7109		85.05942	
			9.9746		9.383861	3.1373		84.48343133	1.601		82.43257	

Appendix A (continued)

HT_09	Fellow	**Metal**	6.4457	1.115624198	8.078662	2.0703	0.343785314	90.54653665	1.0892	0.164996627	81.94009	3
			6.7579		5.551158	2.4752		84.50990149	1.0786		89.18143	
			8.971		6.371085	2.7156		92.86383947	0.9916		84.31362	
			6.1675		1.406492	1.8332		90.63711184	1.3163		91.25387	
			7.3683		6.285958	2.2308		86.23624898	0.8659		84.97264	
		Ceramic										
HT_10	Attending	**Metal**		1.761199895			0.267597327			0.22518488		1
			9.2388		1.82838	1.512		89.85557503	0.7695		88.17734	
			5.3489		1.722459	1.0369		88.29950197	0.2342		90.2741	
			6.1265		2.023	0.9226		88.47356966	0.42		91.32729	
			5.8519		1.547759	0.9962		90.11255515	0.3981		91.54366	
		Ceramic	6.1004	1.302055833	3.374496	1.4669	0.613364728	93.37444373	0.6009	0.65550224	90.01875	1
			9.6163		5.759613	2.8295		95.75877713	0.6852		90.09781	
			7.7718		4.82308	2.4392		92.63452721	1.8533		85.96288	
			7.7679		8.267664	1.9465		96.06536995	1.8		95.59725	
			8.6749		4.962629	1.4179		94.9576474	0.6095		89.77825	
HT_11	Fellow	**Metal**	5.25	0.764702777	6.628411	0.7985	0.205166372	83.63872354	0.4459	0.118456249	91.85514	3
			4.4611		7.117951	1.1148		85.68958978	0.6262		95.65368	
			4.6345		6.598906	1.1126		86.00052256	0.609		95.24023	
			5.8664		6.633363	0.645		84.88737743	0.7352		94.21517	
			6.2326		7.202473	0.9786		84.2692357	0.7335		94.34821	
		Ceramic	3.954	0.634406867	9.723068	0.5924	0.110201897	82.49023437	0.866	0.178593995	83.85966	3
			5.0012		6.439563	0.8862		83.61624422	1.0969		89.15754	
			3.7465		8.693378	0.7723		83.24804724	0.7457		84.5495	
			3.3446		8.425655	0.6712		81.62604083	0.6414		90.92529	
			4.3859		9.25142	0.7306		81.51070278	0.712		86.3499	
HT_12	Attending	**Metal**	9.0975	0.483385762	4.638868	1.9451	0.172702423	85.55432308	0.3343	0.195002518	91.32212	3
			8.4818		4.981683	1.5358		85.39467008	0.3169		91.89541	
			9.1731		4.227996	1.92		86.46712667	0.3165		92.31972	
			9.0828		4.537187	1.6635		86.18515752	0.7079		92.45259	
			9.8438		4.495149	1.762		86.91443214	0.644		93.26572	
		Ceramic	7.4204	0.791955533	7.249758	1.5284	0.580158705	83.84820506	1.1638	0.133985951	86.17883	3
			7.7271		9.124994	1.3172		83.90322277	0.9257		83.23647	
			9.0079		10.03437	2.2119		82.60694945	1.0747		83.25323	
			8.9349		13.69956	2.7383		76.71126677	0.8199		86.72989	
			9.0676		11.20855	1.6364		80.87677367	1.0394		83.54392	
HT_13	Attending	**Metal**	10.0728	0.690382338	3.572567	3.3334	0.382358506	91.13947192	2.2246	0.571505151	93.38553	1
			10.7932		4.253565	3.3257		89.04229156	2.2081		94.14396	
			10.9085		2.076232	2.4613		88.5558611	0.9133		91.49139	
			11.7088		3.030762	2.7322		88.14963045	1.9663		92.39951	
			11.7075		3.154959	3.0808		87.11182072	2.2595		91.26864	
		Ceramic	11.2979	2.228559285	6.335625	3.5817	0.566355155	92.39488361	2.0112	0.770838175	95.86212	1
			12.524		0.900053	3.8221		89.21182082	2.6463		89.56544	
			10.9454		1.193719	3.3261		88.82341431	1.5626		90.20149	
			11.8781		2.034146	3.2705		91.22163485	2.3832		88.37379	
			16.4611		7.786062	4.6672		97.41271135	3.6136		92.36882	
HT_14	Attending	**Metal**	5.7131	0.789001136	9.898271	2.1928	0.22559697	80.11895724	0.5914	0.592822187	90.57796	1
			6.7188		4.873717	1.927		85.32665179	0.5769		88.61998	
			6.7348		5.992599	2.2143		84.13649837	1.0904		88.76715	
			7.9402		3.80857	2.562		91.77075582	1.9751		93.37081	
			6.774		5.823412	2.2157		84.38947862	0.6802		91.5552	
		Ceramic		1.62423961			0.465974001			0.303976144		1
			10.081		3.284749	2.2177		93.24226793	1.0117		90.52601	
			12.3208		3.040302	3.0337		90.30463367	1.5011		86.97503	
			10.2691		2.311552	2.2458		92.13233215	1.5038		90.89202	
			8.3533		4.963909	1.9547		94.68811296	0.9445		91.62792	
HT_15	R1	**Metal**	7.4799	1.031443232	3.053394	1.6527	0.385483132	88.48530349	0.9802	0.168320967	92.65059	1
			7.2804		7.499843	1.2454		82.68712527	1.3714		91.65515	
			8.706		2.69097	2.2711		90.43914255	0.975		92.65484	
			9.602		2.702913	1.9104		91.43124778	1		92.2924	
			9.1942		1.19169	1.5619		89.3725879	1.0456		91.01311	
		Ceramic	7.4924	2.313715016	4.638681	2.4263	0.336674712	93.5870343	1.2776	0.410047756	92.93733	1
			8.4889		5.562302	1.6035		94.95174241	0.5817		92.52735	
			12.2265		6.461115	2.0226		93.9359171	1.6509		95.11583	
			11.4982		5.144861	1.7839		92.28107616	1.4083		94.60909	
			7.2663		5.374394	2.2631		93.91100266	1.0031		93.68048	

Appendix A (continued)

HT_16	R5	**Metal**										
		Ceramic	8.45	1.393756128	10.6769	2.4078	0.723356422	79.37270198	0.6868	0.283399017	88.98381	3
			6.8415		3.926693	1.3076		86.12446603	0.5413		89.36918	
			9.9308		9.574128	3.2053		80.51446213	0.9976		91.28756	
			9.9669		7.414415	2.9043		82.69780795	0.6684		88.72183	
			10.0075		4.493584	2.3478		86.09749282	1.2341		87.77573	
HT_17	R1	**Metal**										
		Ceramic	3.8307	1.372593708	4.166341	0.8142	0.566559779	86.12596446	0.7451	0.429593294	88.46929	15
			6.4379		12.99684	2.2363		80.15600689	1.3926		98.40181	
			7.0416		2.74444	2.1286		88.15638229	1.5881		87.96772	
			7.014		3.09848	1.5261		90.56527762	1.7065		86.95362	
			6.9114		3.243077	1.6731		87.24277379	1.8415		88.29391	
HT_18	R1	**Metal**	8.5935	1.326061246	3.726236	3.2931	0.308354047	93.72378047	0.7376	0.394836665	89.86494	1
			9.0846		4.6857	3.4163		94.67556206	1.4132		90.30738	
			10.4002		1.988361	3.2961		91.81556165	1.3662		90.81048	
			11.8487		4.955216	2.6481		94.75120626	0.874		88.59603	
			10.8769		2.114552	3.0202		90.80437634	0.5144		91.95546	
		Ceramic										
HT_22	Fellow	**Metal**										
		Ceramic	12.0351	1.541567337	3.097221	3.8198	0.91182027	90.93653423	2.4373	0.34171542	92.95197	1
			11.3748		5.374764	3.4144		95.17592926	1.7486		91.44445	
			14.8298		6.144821	5.7143		96.13368298	2.3485		90.36839	
			11.6051		1.134874	3.6787		89.5083532	1.8801		91.02283	
			10.9609		9.855518	4.2473		99.0795501	1.7167		93.80102	
HT_23	Fellow	**Metal**										
		Ceramic	8.364	1.263777426	11.00354	2.9462	0.417184716	79.14735533	1.4531	0.580288945	88.20565	3
			9.6891		7.955183	2.2505		82.07075542	2.1375		89.36221	
			9.7066		8.050425	2.5675		82.97591901	2.7954		86.08634	
			11.6578		7.967051	3.2214		93.80859614	2.8821		96.98737	
			10.8947		7.354333	3.1833		82.64906123	2.4759		90.22219	
HT_24_L	Attending	**Metal**	9.5532	1.108135126	1.715005	1.6441	0.326661014	88.83631731	1.3747	0.208827773	88.74038	5
			11.3945		2.585527	2.1449		87.60622611	1.5691		89.02343	
			9.846		2.009731	1.4163		88.42784224	1.0273		88.74838	
			9.2476		3.62985	1.6363		89.04834384	1.4268		86.49744	
			11.6604		2.948845	2.1312		88.20514351	1.48996		87.66107	
		Ceramic	7.4064	1.401683401	3.970326	1.194	0.293175434	92.91612697	1.5787	0.272839352	87.30795	3
			7.6203		3.872841	1.2711		92.70460444	1.1139		92.76994	
			9.5119		3.66228	1.7224		92.44252513	1.5988		87.27285	
			8.4533		1.307147	1.7199		88.69615528	1.4641		90.09283	
			5.7189		1.215609	1.1196		89.74257723	1.0111		91.18803	
HT_24_R	Attending	**Metal**	10.4634	0.997302736	3.438532	1.3479	0.258649148	88.60275957	1.6019	0.232216985	86.85877	5
			10.9463		3.340738	1.7187		88.89999309	0.9976		86.84594	
			11.2607		2.845215	1.2149		87.50860196	1.3779		88.62675	
			11.0494		3.526941	1.2293		86.71998452	1.2195		88.70495	
			8.7978		4.235197	1.0208		85.85730095	1.1389		89.12123	
		Ceramic	8.6015	0.69063414	4.139658	1.2585	0.158221828	87.57962296	0.8411	0.16855548	93.35635	3
			7.7946		6.202529	1.287		86.23969614	1.0884		85.07441	
			9.104		3.970481	1.1529		87.62295591	1.2747		86.82152	
			9.5886		11.30653	1.2526		93.09704868	0.9645		100.8633	
			8.3443		4.421569	1.5729		87.01515397	1.1593		86.74091	

Appendix A (continued)

		Metal	8.8737	1.468563335	1.684325	1.5695	0.212233426	91.31673568	0.5626	0.27232286	88.94987	
			6.8219		2.998026	1.2696		88.50269551	0.4608		87.40324	
			9.3513		2.233867	1.5659		90.97350569	0.705		87.98961	3
			6.0953		4.29718	1.0668		85.72355811	0.953		90.42088	
			6.558		3.718113	1.3693		91.4578716	1.1176		86.58036	
HT_25	Attending	**Ceramic**	7.8022	0.913431346	1.761644	3.0324	0.221618302	91.68919496	1.1602	0.232311166	89.50013	
			8.1083		8.885428	2.9576		98.24073361	0.5476		93.29989	
			9.9458		2.481569	3.5		87.61427331	0.6826		90.68261	3
			8.2739		5.91175	3.2515		88.70011283	0.9007		95.76607	
			9.3691		7.073253	3.3346		93.42669868	0.8496		96.18036	
		Metal										
HT_26	Attending	**Ceramic**	7.0431	0.792973899	5.569059	1.5278	0.707628778	89.21703198	0.6861	0.244274299	84.4866	
			6.8572		9.722275	1.5064		89.1665318	1.1705		80.31421	
			7.7416		4.766917	2.1379		90.11210654	1.1922		85.23441	3
			7.174		4.873677	1.1294		89.06015212	0.8728		85.21823	
			8.8161		5.017972	2.9358		94.98550773	0.7077		89.43157	
		Metal										
HT_27	Attending	**Ceramic**	5.3845	0.826797333	7.151634	1.0856	0.178862005	83.863528	0.906	0.25217099	86.34125	
			6.0769		4.980305	1.1391		85.04849871	1.1944		89.46648	
			7.0811		8.068099	1.0362		85.50506913	1.5657		83.31384	5
			6.373		7.765581	0.8791		86.26135556	1.3954		83.20334	
			7.4795		4.723523	1.3709		93.90417774	1.3932		87.34535	
		Metal	17.82549	2.781227411	3.355834	3.0854	0.575750413	92.25248054	0.8476	0.171182987	87.51372	
			12.99343		2.428497	1.8837		89.31843206	0.5785		87.66922	
			13.62026		1.654733	1.7527		88.40823907	0.7863		89.54797	1
			16.00255		3.302901	1.6679		92.35444986	0.8561		87.6849	
			10.62836		3.819981	2.1301		93.79541097	0.478		89.56807	
HT_28	R4	**Ceramic**	12.2165	2.045819705	2.216979	1.9802	0.987844559	90.2104253	1.5689	0.366964648	92.20696	
			10.1628		7.379657	2.4323		93.540858	1.2148		96.4664	
			15.6633		3.747471	3.6408		92.18039107	1.8642		93.04638	1
			13.364		13.14442	3.4673		102.452017	2.1975		94.14354	
			13.9358		8.998843	4.4492		97.20047051	1.8343		95.36893	
		Metal	5.4977	0.709218117	1.124695	1.9046	0.20751879	88.89439434	0.6847	0.26306215	90.20631	
			5.871		5.916324	2.2543		84.62114453	0.7442		87.54334	
			6.8374		4.077344	2.0486		86.19657371	0.8413		91.46709	3
			7.0144		1.033366	1.8915		89.17755692	0.7704		90.6256	
			5.4346		8.525681	1.8424		81.51750896	0.6031		90.85082	
HT_29	R5	**Ceramic**	8.839	0.833297548	4.280235	1.6688	0.226951587	85.84577724	1.4799	0.438147949	88.97086	
			8.1584		0.913263	1.8383		90.90377229	1.9592		89.86869	
			9.0581		6.362802	1.8244		83.69332865	1.2181		90.83989	3
			8.5505		6.524995	2.0855		83.54592965	0.916		89.04461	
			6.9472		3.370375	1.4718		87.12133641	0.9168		91.75144	
		Metal	15.3141	3.298641916	9.898816	2.3153	0.641295301	86.54184243	3.2197	1.293987421	80.73629	
			12.6043		8.652372	1.8301		83.3718573	1.44795		84.46332	
			13.9747		5.209421	2.8908		85.46514507	4.45		87.44154	1
			11.0788		10.088	3.4768		81.06144916	2.0975		85.36148	
			6.7615		15.05055	3.0173		75.62996093	1.4448		85.61938	
HT_30	R4	**Ceramic**	13.89335	1.297588238	7.43314	4.2792	0.743906227	82.57924504	1.1364	0.661325595	90.42652	
			10.86827		3.101795	2.916		90.48483092	2.7176		93.0636	
			11.00263		3.897413	3.6096		91.39302911	2.2276		93.63924	1
			12.82174		2.250201	2.8089		87.75611133	1.9796		90.16834	
			12.74357		6.176974	2.3953		84.23341921	1.2759		87.79353	
		Metal										
HT_31		**Ceramic**	11.1932	0.474177717	7.001684	1.9102	0.445637405	85.36140056	1.6394	0.241285377	84.76679	
			10.6012		9.500463	2.3132		81.24523916	1.848		86.33917	
			9.9013		8.378693	3.0065		83.94492791	1.6091		84.2304	3
			10.2757		6.631074	2.6495		84.37543384	1.3233		86.49912	
			10.484		7.989402	2.8827		83.09378278	1.2635		86.00268	
		Metal										
HT_32		**Ceramic**	5.0582	1.102303492	3.049269	1.7891	0.423578555	92.73497209	0.6191	0.223118988	88.6527	
			7.5464		5.653821	2.7952		91.77961347	1.0778		95.36471	
			5.097		5.868649	1.7864		92.08257739	0.6104		95.48428	1
			6.7144		6.523889	2.287		94.71485513	0.7803		94.49882	
			5.4922		5.401256	2.0024		95.16879493	0.5072		91.56327	

Table 9: Raw impaction force and angle data for each subject

Appendix B

Number	Level	M/C	Max Fz (kN	θz (deg)	Max Fx (kN	θx (deg)	Max Fy (kN	θy (deg)	# Hits
HT_01	Fellow	Metal	2.6613	4.849157	0.535375	91.62546	0.507875	94.38573	3
		Ceramic	2.74634	11.29576	0.6285	79.96725	0.36344	84.88456	3
HT_02	R3	Metal	3.621925	7.36106	0.9361	83.01736	1.5251	89.12828	1
		Ceramic	5.71142	5.092504	1.38274	85.92817	1.54826	89.79933	1
HT_04	R5	Metal							
		Ceramic	6.07632	4.792853	1.09158	88.11065	0.3832	91.50451	3
HT_05	R4	Metal	10.44948	3.425713	2.1437	91.15926	1.11928	92.81525	5
		Ceramic	8.96064	7.001806	1.60758	85.7262	1.7736	85.35764	3
HT_06	R2	Metal	6.76026	2.620725	2.07446	92.04471	0.88368	90.95567	2
		Ceramic							
HT_07	Fellow	Metal							
		Ceramic	5.88606	8.88864	1.35422	89.39523	1.46578	82.07171	2
HT_08	Attending	Metal	7.92014	4.732766	1.36232	86.66045	2.20578	93.12074	2
		Ceramic	8.75816	7.393306	2.78344	86.71889	1.65466	85.61882	2
HT_09	Fellow	Metal	7.14208	5.538671	2.26502	88.95873	1.06832	86.33233	3
		Ceramic							
HT_10	Attending	Metal	6.641525	1.7804	1.116925	89.1853	0.45545	90.3306	1
		Ceramic	7.98626	5.437496	2.02	94.55815	1.10978	90.29099	1
HT_11	Fellow	Metal	5.28892	6.836221	0.9299	84.89709	0.62996	94.26249	3
		Ceramic	4.08644	8.506617	0.73054	82.49825	0.8124	86.96838	3
HT_12	Attending	Metal	9.1358	4.576177	1.76528	86.10314	0.46392	92.25111	3
		Ceramic	8.43158	10.26345	1.88644	81.58928	1.0047	84.58847	3
HT_13	Attending	Metal	11.03816	3.217617	2.98668	88.79982	1.91436	92.53781	1
		Ceramic	12.6213	3.649921	3.73352	91.81289	2.44338	91.27433	1
HT_14	Attending	Metal	6.77618	6.079314	2.22236	85.14847	0.9828	90.57822	1
		Ceramic	10.25605	3.400128	2.362975	92.59184	1.240275	90.00524	1
HT_15	R1	Metal	8.4525	3.427762	1.7283	88.48308	1.07444	92.05322	1
		Ceramic	9.39446	5.43627	2.01988	93.73335	1.18432	93.77402	1

Appendix B (continued)

HT_16	R5	**Metal**							
		Ceramic	9.03934	7.217144	2.43456	82.96139	0.82564	89.22762	3
HT_17	R1	**Metal**							
		Ceramic	6.24712	5.249835	1.67566	86.44928	1.45476	90.01727	15
HT_18	R1	**Metal**	10.16078	3.494013	3.13476	93.1541	0.98108	90.30686	1
		Ceramic							
HT_22	Fellow	**Metal**							
		Ceramic	12.16114	5.12144	4.1749	94.16681	2.02624	91.91773	1
HT_23	Fellow	**Metal**							
		Ceramic	10.06244	8.466107	2.83378	84.13034	2.3488	90.17275	3
HT_24_L	Attedning	**Metal**	10.34034	2.577792	1.79456	88.42477	1.377572	88.13414	5
		Ceramic	7.74216	2.805641	1.4054	91.3004	1.35332	89.72632	3
HT_24_R	Attending	**Metal**	10.50352	3.477325	1.30632	87.51773	1.26716	88.03153	5
		Ceramic	8.6866	6.008154	1.30478	88.3109	1.0656	90.5713	3
HT_25	Attending	**Metal**	7.54004	2.986302	1.36822	89.59487	0.7598	88.26879	3
		Ceramic	8.69986	5.222729	3.21522	91.9342	0.82814	93.08581	3
HT_26	Attending	**Metal**							
		Ceramic	7.5264	5.98998	1.84746	90.50827	0.92586	84.937	3
HT_27	Attedning	**Metal**							
		Ceramic	6.479	6.537828	1.10218	86.91653	1.29094	85.93405	5
HT_28	R4	**Metal**	14.21402	2.912389	2.10396	91.2258	0.7093	88.39678	1
		Ceramic	13.06848	7.097474	3.19396	95.11683	1.73594	94.24644	1
HT_29	R5	**Metal**	6.13102	4.135482	1.98828	86.08144	0.72874	90.13863	3
		Ceramic	8.31064	4.290334	1.77776	86.22203	1.298	90.0951	3
HT_30	R4	**Metal**	11.94668	9.779833	2.70606	82.41405	2.53199	84.7244	1
		Ceramic	12.26591	4.571904	3.2018	87.28933	1.86742	91.01825	1
HT_31	R3	**Metal**							
		Ceramic	10.49108	7.900263	2.55242	83.60416	1.53666	85.56763	3
HT_32	R1	**Metal**							
		Ceramic	5.98164	5.299377	2.13202	93.29616	0.71896	93.11275	1

Table 10: Summary of average data for each surgeon

Appendix C

Number	Level	M/C	Max Fz (kN)	p	Max Fx (kN)	p	Max Fy (kN)	p
HT_01	Fellow	Metal	2.6613		0.535375		0.507875	
		Ceramic	2.74634	0.738	0.6285	0.216	0.36344	0.071
HT_02	R3	Metal	3.621925		0.9361		1.5251	
		Ceramic	5.71142	0.015	1.38274	0.123	1.54826	0.936
HT_03	M3	Metal	2.89264		0.68924		0.4049	
		Ceramic						
HT_04	R5	Metal						
		Ceramic	6.07632		1.09158		0.3832	
HT_05	R4	Metal	10.44948		2.1437		1.11928	
		Ceramic	8.96064	0.007	1.60758	0.008	1.7736	0.039
HT_06	R2	Metal	6.76026		2.07446		0.88368	
		Ceramic						
HT_07	Fellow	Metal						
		Ceramic	5.88606		1.35422		1.46578	
HT_08	Attending	Metal	7.92014		1.36232		2.20578	
		Ceramic	8.75816	0.289	2.78344	0.001	1.65466	0.054
HT_09	Fellow	Metal	7.14208		2.26502		1.06832	
		Ceramic						
HT_10	Attending	Metal	6.641525		1.116925		0.45545	
		Ceramic	7.98626	0.228	2.02	0.03	1.10978	0.101
HT_11	Fellow	Metal	5.28892		0.9299		0.62996	
		Ceramic	4.08644	0.027	0.73054	0.092	0.8124	0.093
HT_12	Attending	Metal	9.1358		1.76528		0.46392	
		Ceramic	8.43158	0.128	1.88644	0.666	1.0047	0.001
HT_13	Attending	Metal	11.03816		2.98668		1.91436	
		Ceramic	12.6213	168	3.73352	0.04	2.44338	0.253
HT_14	Attending	Metal	6.77618		2.22236		0.9828	
		Ceramic	10.25605	0.004	2.362975	0.568	1.240275	0.459
HT_15	R1	Metal	8.4525		1.7283		1.07444	
		Ceramic	9.39446	0.43	2.01988	0.238	1.18432	0.595
HT_16	R5	Metal						
		Ceramic	9.03934		2.43456		0.82564	

Appendix C (continued)

HT_17	R1	**Metal**						
		Ceramic	6.24712		1.67566		1.45476	
HT_18	R1	**Metal**	10.16078		3.13476		0.98108	
		Ceramic						
HT_19	M4	**Metal**						
		Ceramic	6.1942		1.87906		1.31248	
HT_20	M4	**Metal**	10.7715		2.54824		1.52936	
		Ceramic						
HT_21	M4	**Metal**	8.52222		2.03384		1.52158	
		Ceramic						
HT_22	Fellow	**Metal**						
		Ceramic	12.16114		4.1749		2.02624	
HT_23	Fellow	**Metal**						
		Ceramic	10.06244		2.83378		2.3488	
HT_24_L	Attending	**Metal**	10.34034		1.79456		1.377572	
		Ceramic	7.74216	0.012	1.4054	0.083	1.35332	0.878
HT_24_R	Attending	**Metal**	10.50352		1.30632		1.26716	
		Ceramic	8.6866	0.01	1.30478	0.991	1.0656	0.158
HT_25	Attending	**Metal**	7.54004		1.36822		0.7598	
		Ceramic	8.69986	0.172	3.21522	0.00000009	0.82814	0.681
HT_26	Attending	**Metal**						
		Ceramic	7.5264		1.84746		0.92586	
HT_27	Attending	**Metal**						
		Ceramic	6.479		1.10218		1.29094	
HT_28	R4	**Metal**	14.214018		2.10396		0.7093	
		Ceramic	13.06848	0.479	3.19396	0.066	1.73594	0.00005
HT_29	R5	**Metal**	6.13102		1.98828		0.72874	
		Ceramic	8.31064	0.002	1.77776	0.134	1.298	0.022
HT_30	R4	**Metal**	11.94668		2.70606		2.53199	
		Ceramic	12.265912	0.845	3.2018	0.292	1.86742	0.346
HT_31	R3	**Metal**						
		Ceramic	10.49108		2.55242		1.53666	
HT_32	R1	**Metal**						
		Ceramic	5.98164		2.13202		0.71896	

Table 11: Force data for each surgeon with significant differences highlighted in green

Appendix D

Number	Level	M/C	θz (deg)	p	θx (deg)	p	θy (deg)	p
HT_01	Fellow	**Metal**	4.849157		91.62546		94.38573	
		Ceramic	11.29576	0.001	79.96725	0.000014	84.88456	6E-07
HT_02	R3	**Metal**	7.36106		83.01736		89.12828	
		Ceramic	5.092504	0.202	85.92817	0.21	89.79933	0.672
HT_03	M3	**Metal**	3.972907		91.05198		90.5308	
		Ceramic						
HT_04	R5	**Metal**						
		Ceramic	4.792853		88.11065		91.50451	
HT_05	R4	**Metal**	3.425713		91.15926		92.81525	
		Ceramic	7.001806	0.036	85.7262	0.002	85.35764	0.004
HT_06	R2	**Metal**	2.620725		92.04471		90.95567	
		Ceramic						
HT_07	Fellow	**Metal**						
		Ceramic	8.88864		89.39523		82.07171	
HT_08	Attending	**Metal**	4.732766		86.66045		93.12074	
		Ceramic	7.393306	0.229	86.71889	0.98	85.61882	0.014
HT_09	Fellow	**Metal**	5.538671		88.95873		86.33233	
		Ceramic						
HT_10	Attending	**Metal**	1.7804		89.1853		90.3306	
		Ceramic	5.437496	0.005	94.55815	0.00004	90.29099	0.984
HT_11	Fellow	**Metal**	6.836221		84.89709		94.26249	
		Ceramic	8.506617	0.02	82.49825	0.004	86.96838	0.001
HT_12	Attending	**Metal**	4.576177		86.10314		92.25111	
		Ceramic	10.26345	0.001	81.58928	0.011	84.58847	0.000016
HT_13	Attending	**Metal**	3.217617		88.79982		92.53781	
		Ceramic	3.649921	0.776	91.81289	0.111	91.27433	0.402
HT_14	Attending	**Metal**	6.079314		85.14847		90.57822	
		Ceramic	3.400128	0.073	92.59184	0.014	90.00524	0.686
HT_15	R1	**Metal**	3.427762		88.48308		92.05322	
		Ceramic	5.43627	0.108	93.73335	0.011	93.77402	0.018
HT_16	R5	**Metal**						
		Ceramic	7.217144		82.96139		89.22762	

Appendix D (continued)

HT_17	R1	**Metal**						
		Ceramic	5.249835		86.44928		90.01727	
HT_18	R1	**Metal**	3.494013		93.1541		90.30686	
		Ceramic						
HT_19	M4	**Metal**						
		Ceramic	5.611258		88.74165		89.60372	
HT_20	M4	**Metal**	3.527189		87.24362		89.67596	
		Ceramic						
HT_21	M4	**Metal**	4.363564		89.54172		88.55434	
		Ceramic						
HT_22	Fellow	**Metal**						
		Ceramic	5.12144		94.16681		91.91773	
HT_23	Fellow	**Metal**						
		Ceramic	8.466107		84.13034		90.17275	
HT_24_L	Attending	**Metal**	2.577792		88.42477		88.13414	
		Ceramic	2.805641	0.759	91.3004	0.013	89.72632	0.214
HT_24_R	Attending	**Metal**	3.477325		87.51773		88.03153	
		Ceramic	6.008154	0.109	88.3109	0.573	90.5713	0.419
HT_25	Attending	**Metal**	2.986302		89.59487		88.26879	
		Ceramic	5.222729	0.158	91.9342	0.316	93.08581	0.012
HT_26	Attending	**Metal**						
		Ceramic	5.98998		90.50827		84.937	
HT_27	Attending	**Metal**						
		Ceramic	6.537828		86.91653		85.93405	
HT_28	R4	**Metal**	2.912389		91.2258		88.39678	
		Ceramic	7.097474	0.067	95.11683	0.142	94.24644	0.0002
HT_29	R5	**Metal**	4.135482		86.08144		90.13863	
		Ceramic	4.290334	0.932	86.22203	0.945	90.0951	0.961
HT_30	R4	**Metal**	9.779833		82.41405		84.7244	
		Ceramic	4.571904	0.023	87.28933	0.096	91.01825	0.003
HT_31	R3	**Metal**						
		Ceramic	7.900263		83.60416		85.56763	
HT_32	R1	**Metal**						
		Ceramic	5.299377		93.29616		93.11275	

Table 12: Impaction angle data for each surgeon with significant differences highlighted in green

Appendix E

Combined Metal and Ceramic			
	Level	Mean	P-Value
θz	Attending	4.9332	0.01
	Fellow	7.2931	
Fx	Attending	1.9697	0.939
	Fellow	2.0075	
θx	Attending	88.755	0.512
	Fellow	87.6909	
Fy	Attending	1.22	0.695
	Fellow	1.343	
θy	Attending	89.0078	0.706
	Fellow	88.4575	
Fz	Attending	8.5426	0.995
	Resident	8.5489	
θz	Attending	4.9332	0.577
	Resident	5.2954	
Fx	Attending	1.9697	0.575
	Resident	2.1166	
θx	Attending	88.755	0.745
	Resident	88.2938	
Fy	Attending	1.22	0.841
	Resident	1.1795	
θy	Attending	89.0078	0.219
	Resident	90.1128	
Fz	Fellow	7.108	0.331
	Resident	8.5489	
θz	Fellow	7.2931	0.017
	Resident	5.2954	
Fx	Fellow	2.0075	0.81
	Resident	2.1166	
θx	Fellow	87.6909	0.758
	Resident	88.2938	
Fy	Fellow	1.343	0.563
	Resident	1.1795	
θy	Fellow	88.4575	0.215
	Resident	90.1128	

Metal			
	Level	Mean	P-Value
Fz	Attending	8.737	0.017
	Fellow	5.0308	
θz	Attending	3.6785	0.044
	Fellow	5.7413	
Fx	Attending	1.7403	0.315
	Fellow	1.2434	
θx	Attending	87.6793	0.585
	Fellow	88.4938	
Fy	Attending	1.1784	0.291
	Fellow	0.7354	
θy	Attending	90.4066	0.533
	Fellow	91.6602	
Fz	Attending	8.737	0.868
	Resident	8.9671	
θz	Attending	3.6785	0.361
	Resident	4.6446	
Fx	Attending	1.7403	0.272
	Resident	2.102	
θx	Attending	87.6793	0.634
	Resident	88.4475	
Fy	Attending	1.1784	0.96
	Resident	1.1942	
θy	Attending	90.4066	0.617
	Resident	89.8149	
Fz	Fellow	5.0308	0.102
	Resident	8.9671	
θz	Fellow	5.7413	0.498
	Resident	4.6446	
Fx	Fellow	1.2434	0.109
	Resident	2.102	
θx	Fellow	88.4938	0.987
	Resident	88.4475	
Fy	Fellow	0.7354	0.246
	Resident	1.1942	
θy	Fellow	91.6602	0.403
	Resident	89.8149	

Ceramic			
	Level	Mean	P-Value
Fz	Attending	8.7187	0.25
	Fellow	6.9885	
θz	Attending	5.6709	0.037
	Fellow	8.4557	
Fx	Attending	2.1661	0.721
	Fellow	1.9444	
θx	Attending	89.6241	0.166
	Fellow	86.0316	
Fy	Attending	1.2917	0.74
	Fellow	1.4033	
θy	Attending	88.6032	0.459
	Fellow	87.203	
Fz	Attending	8.7187	0.973
	Resident	8.6861	
θz	Attending	5.6709	0.854
	Resident	5.8136	
Fx	Attending	2.1661	0.841
	Resident	2.0973	
θx	Attending	89.6241	0.373
	Resident	88.0398	
Fy	Attending	1.2917	0.959
	Resident	1.3024	
θy	Attending	88.6032	0.198
	Resident	90.3382	
Fz	Fellow	6.9885	0.317
	Resident	8.6861	
θz	Fellow	8.4557	0.008
	Resident	5.8136	
Fx	Fellow	1.9444	0.782
	Resident	2.0973	
θx	Fellow	86.0316	0.436
	Resident	88.0398	
Fy	Fellow	1.4033	0.759
	Resident	1.3024	
θy	Fellow	87.203	0.096
	Resident	90.3382	

Table 13: Statistical p-values comparing surgeon experience levels

Appendix F

Attendings			
	Material	Mean	P-Value
Fz	Metal	8.737	0.982
	Ceramic	8.7187	
θz	Metal	3.6785	0.039
	Ceramic	5.6709	
Fx	Metal	1.7403	0.256
	Ceramic	2.1661	
θx	Metal	87.6793	0.194
	Ceramic	89.6241	
Fy	Metal	1.1784	0.671
	Ceramic	1.2917	
θy	Metal	90.4066	0.173
	Ceramic	88.6032	
Fellows			
	Material	Mean	P-Value
Fz	Metal	5.0308	0.474
	Ceramic	6.9885	
θz	Metal	5.7413	0.097
	Ceramic	8.4557	
Fx	Metal	1.2434	0.504
	Ceramic	1.9444	
θx	Metal	88.4938	0.53
	Ceramic	88.0316	
Fy	Metal	0.7354	0.236
	Ceramic	1.4033	
θy	Metal	91.6602	0.196
	Ceramic	87.203	
Residents			
	Material	Mean	P-Value
Fz	Metal	8.9671	0.839
	Ceramic	8.6861	
θz	Metal	4.6446	0.201
	Ceramic	5.8136	
Fx	Metal	2.102	0.988
	Ceramic	2.0973	
θx	Metal	88.4475	0.835
	Ceramic	88.0398	
Fy	Metal	1.1942	0.667
	Ceramic	1.3024	
θy	Metal	89.8149	0.689
	Ceramic	90.3382	

Table 14: Statistical p-values comparing femoral head material

Appendix G

```
%Attendings Data

x=[PeakDataS8M(1:8,2)];
y=[PeakDataS8M(1:8,3)];

[theta,rho]=cart2pol(x,y);

 %Fellows Data

x2=[PeakDataS8M(9:11,2)];
y2=[PeakDataS8M(9:11,3)];

[theta2,rho2]=cart2pol(x2,y2);

 %Residents Data

x3=[PeakDataS8M(12:19,2)];
y3=[PeakDataS8M(12:19,3)];

[theta3,rho3]=cart2pol(x3,y3);

 %Plot Data Points

polarscatter(theta,rho,'g*')
hold on
polarscatter(theta2,rho2,'b*')
hold on
polarscatter(theta3,rho3,'r*')
hold on

%Rotate and flip axes

polaraxis=gca
polaraxis.ThetaZeroLocation='bottom'
polaraxis.ThetaDir='clockwise'

%Create Legend and Title

legend('Attending','Fellow','Resident')

title('Metal Head Impaction Location')


%Attendings Data

x=[PeakDataS8C(1:10,2)];
y=[PeakDataS8C(1:10,3)];
```

Appendix G (continued)

```
[theta,rho]=cart2pol(x,y);

%Fellows Data

x2=[PeakDataS8C(11:15,2)];
y2=[PeakDataS8C(11:15,3)];

[theta2,rho2]=cart2pol(x2,y2);

 %Residents Data

x3=[PeakDataS8C(16:26,2)];
y3=[PeakDataS8C(16:26,3)];

[theta3,rho3]=cart2pol(x3,y3);

 %Plot Data Points

figure
polarscatter(theta,rho,'g*')
hold on
polarscatter(theta2,rho2,'b*')
hold on
polarscatter(theta3,rho3,'r*')
hold on

%Rotate and flip axes

polaraxis=gca
polaraxis.ThetaZeroLocation='bottom'
polaraxis.ThetaDir='clockwise'

%Create Legend and Title

legend('Attending','Fellow','Resident')

title('Ceramic Head Impaction Location')
```

Appendix H

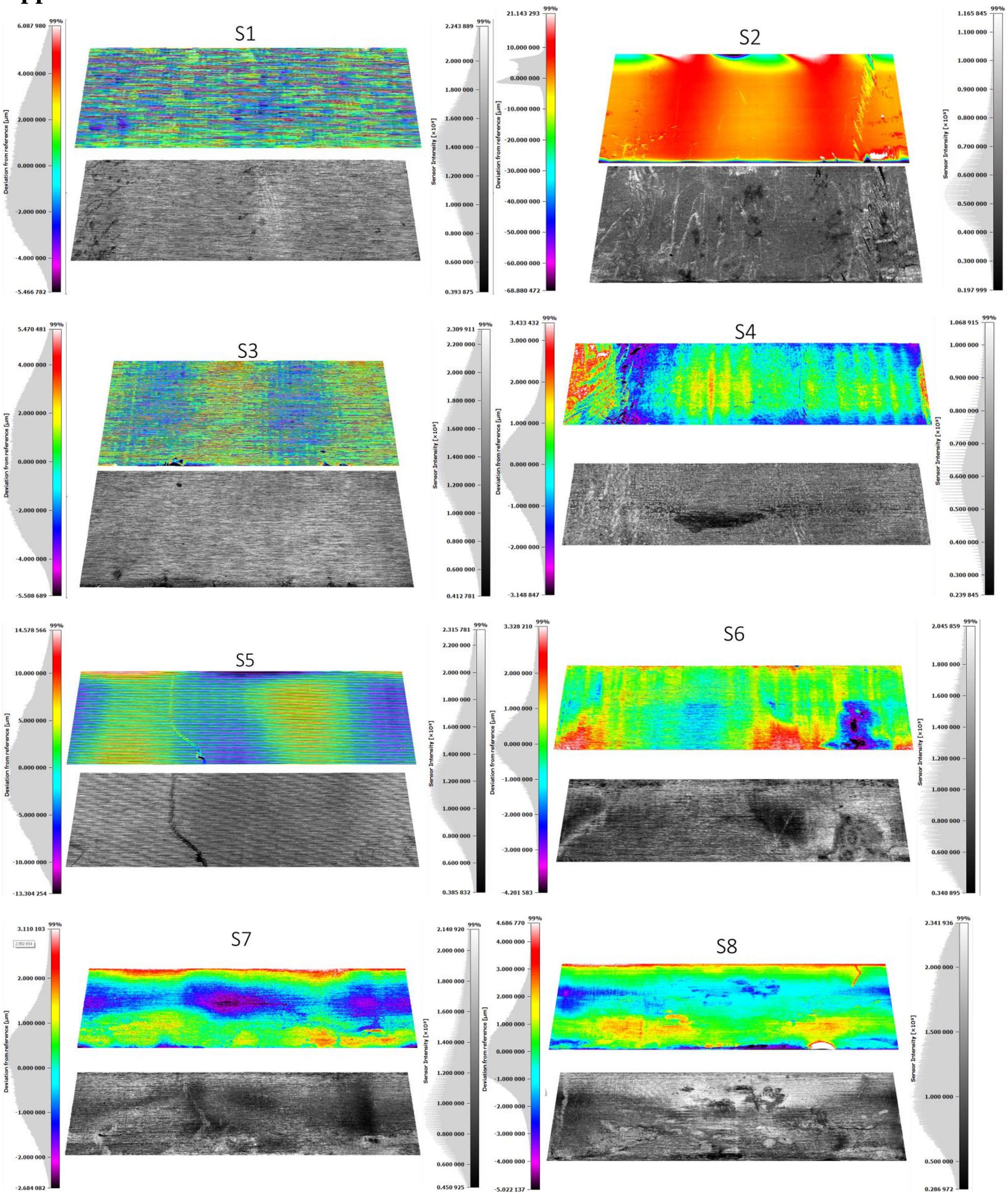

Appendix H (continued)

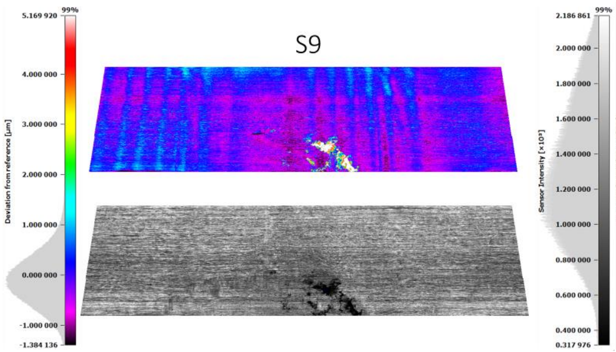

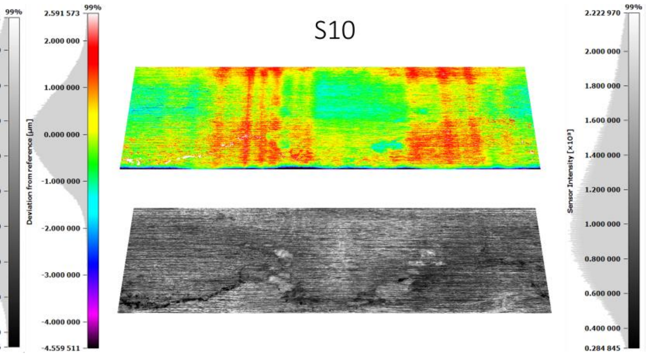

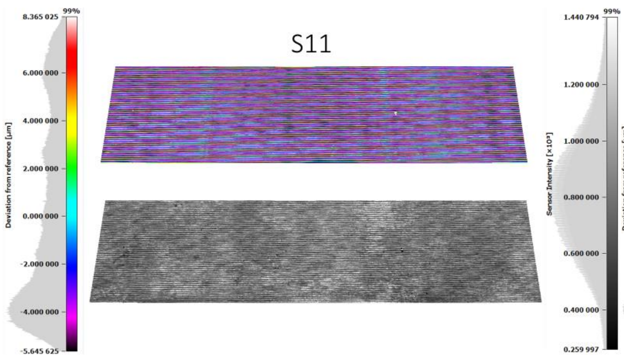

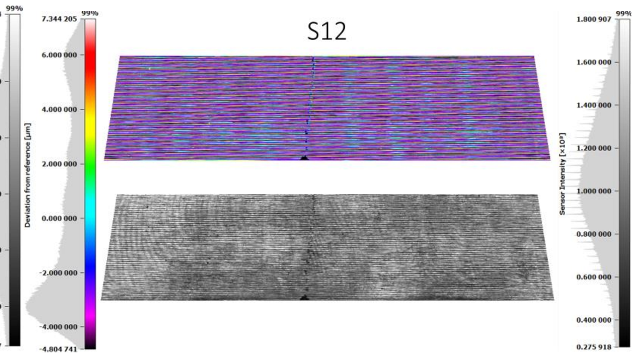

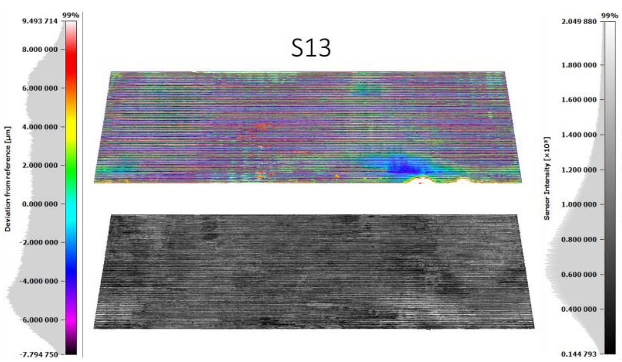

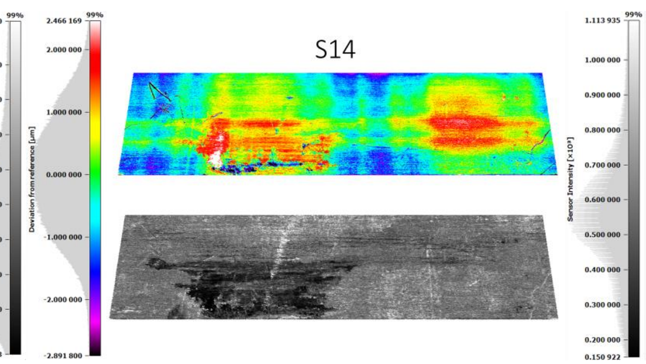

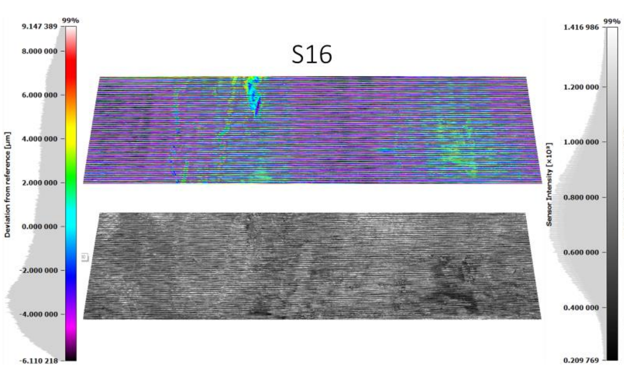

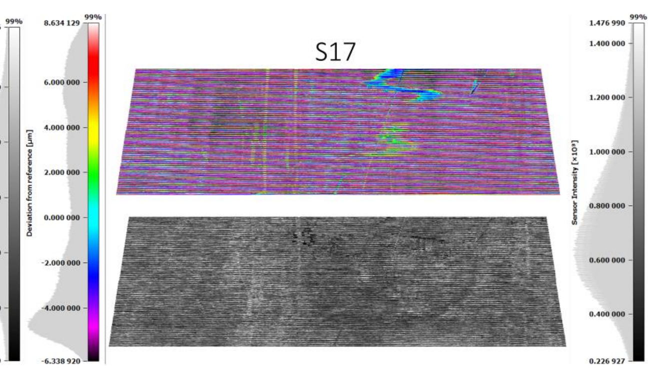

Appendix H (continued)

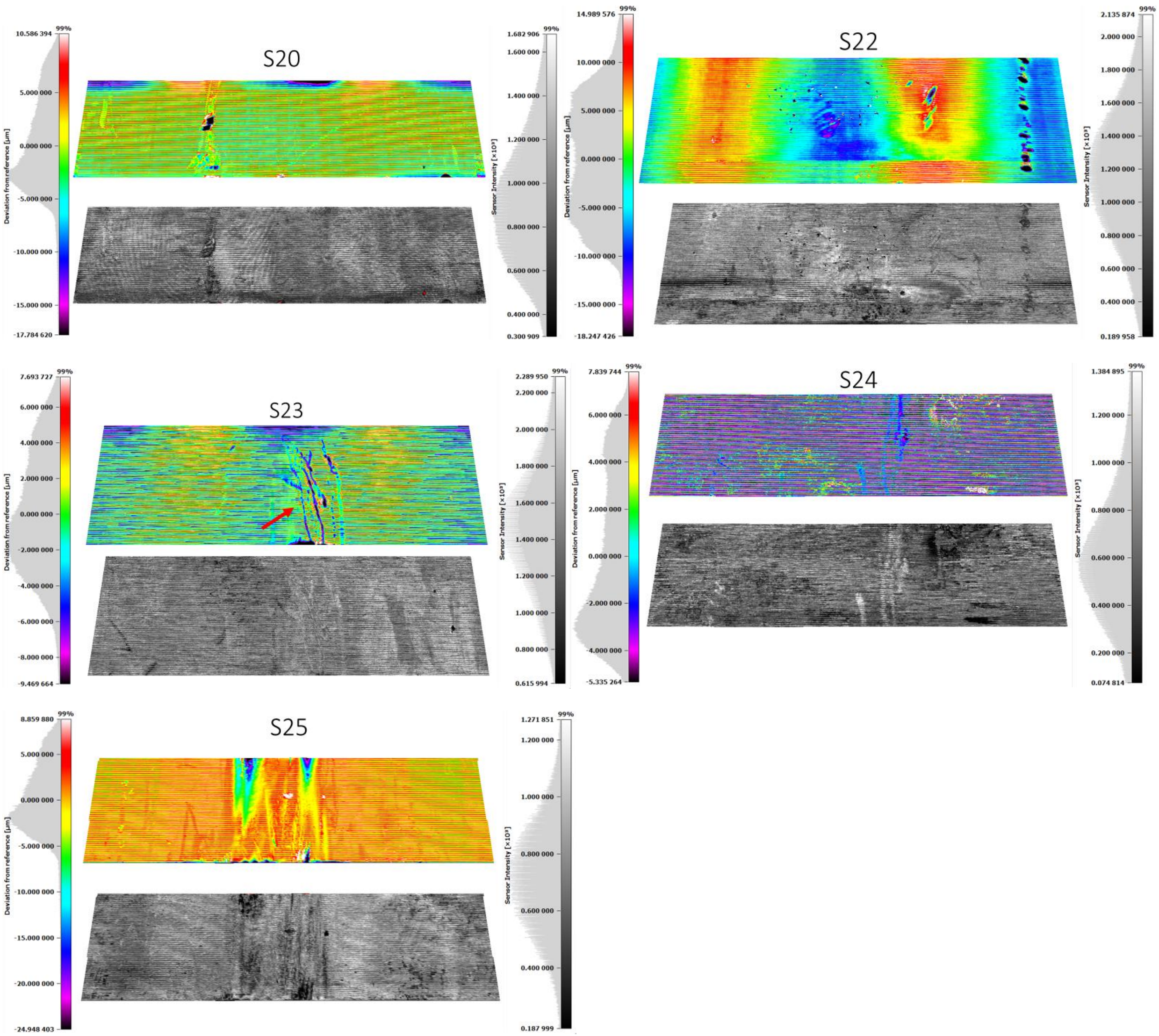

Figure 27: RedLux images for all stem tapers

Appendix I

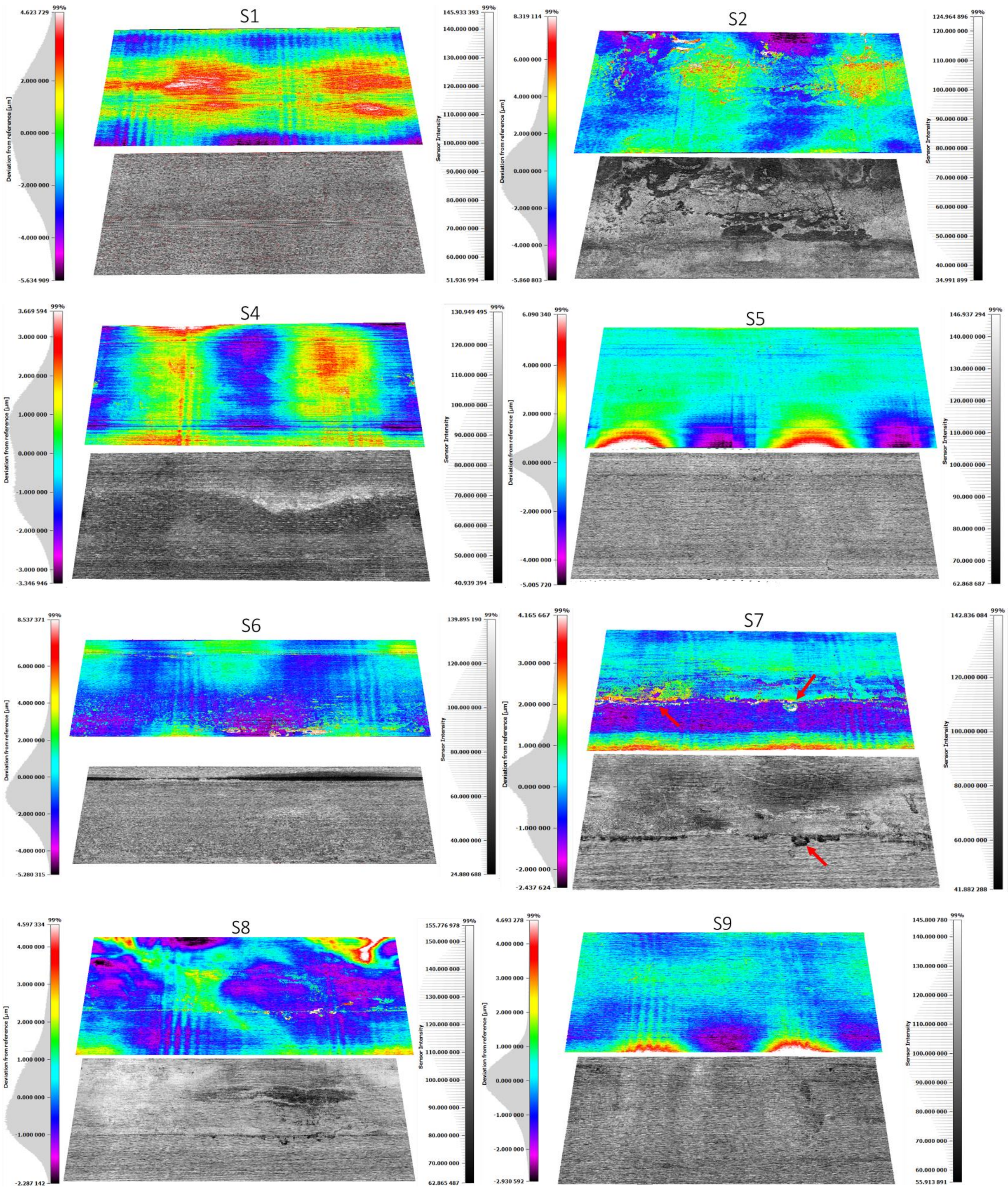
S1
S2
S4
S5
S6
S7
S8
S9
Deviation from reference [µm]
Sensor Intensity
99%

Appendix I (continued)

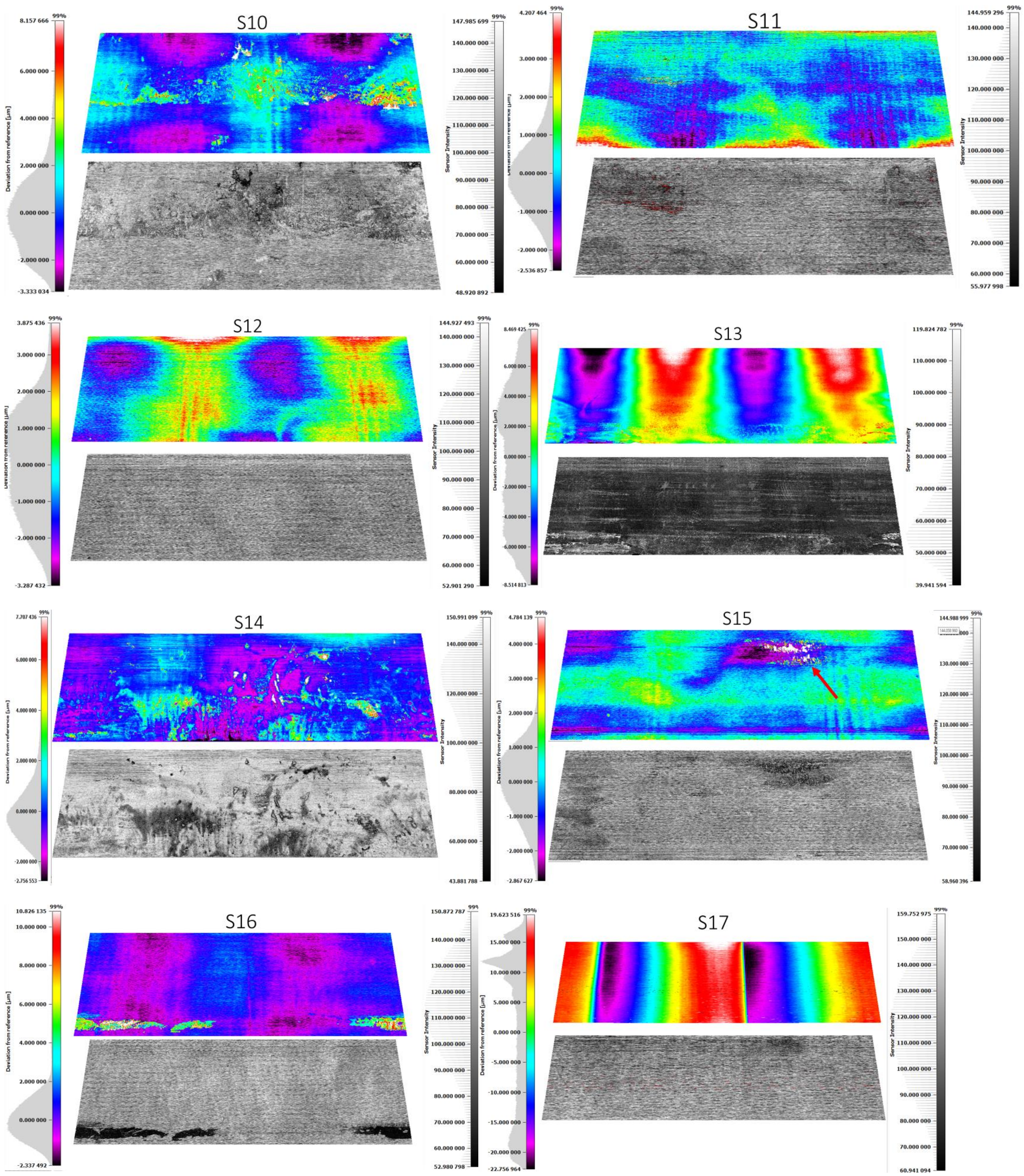

Appendix I (continued)

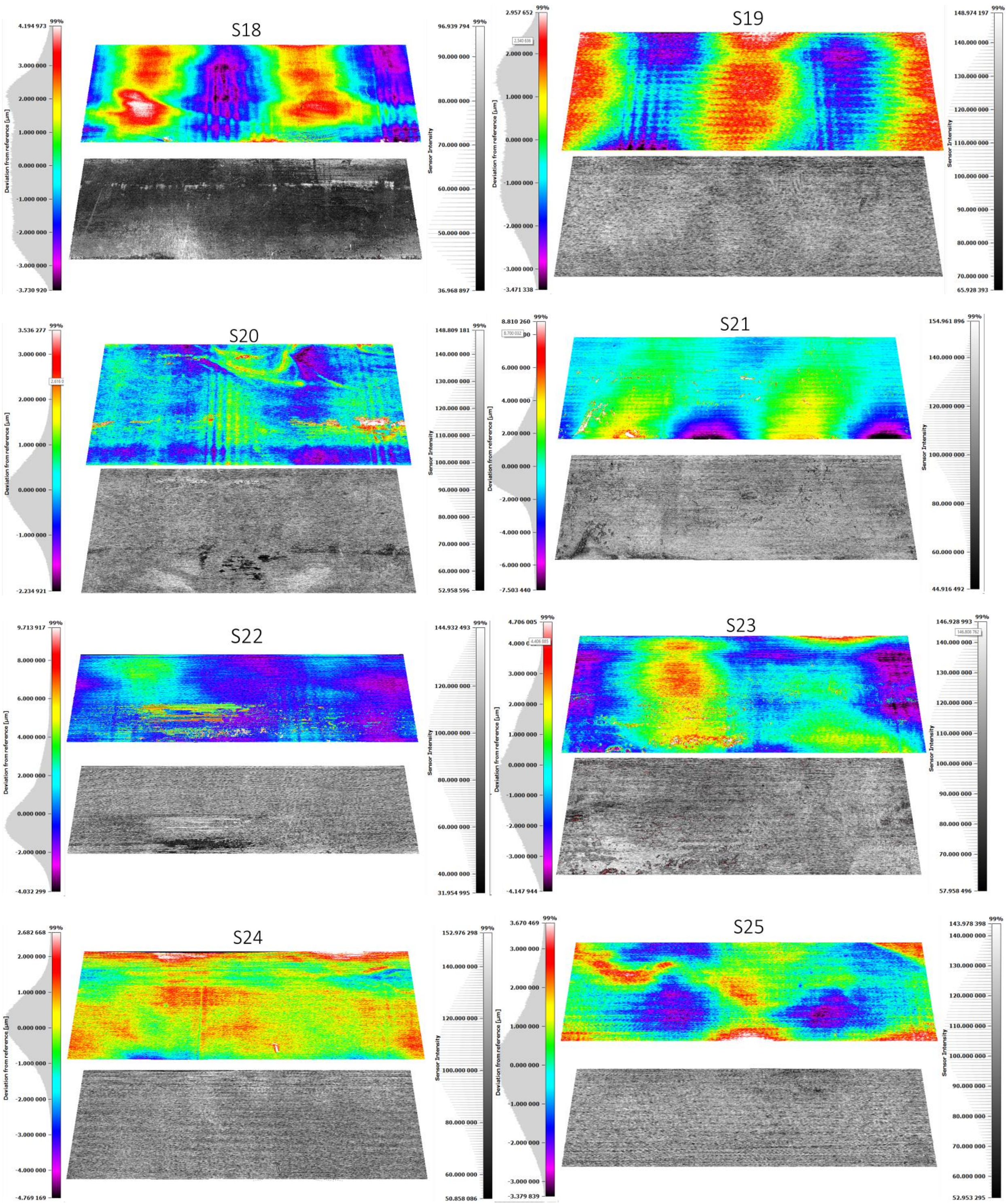

Figure 28: RedLux images for all head tapers

Appendix J

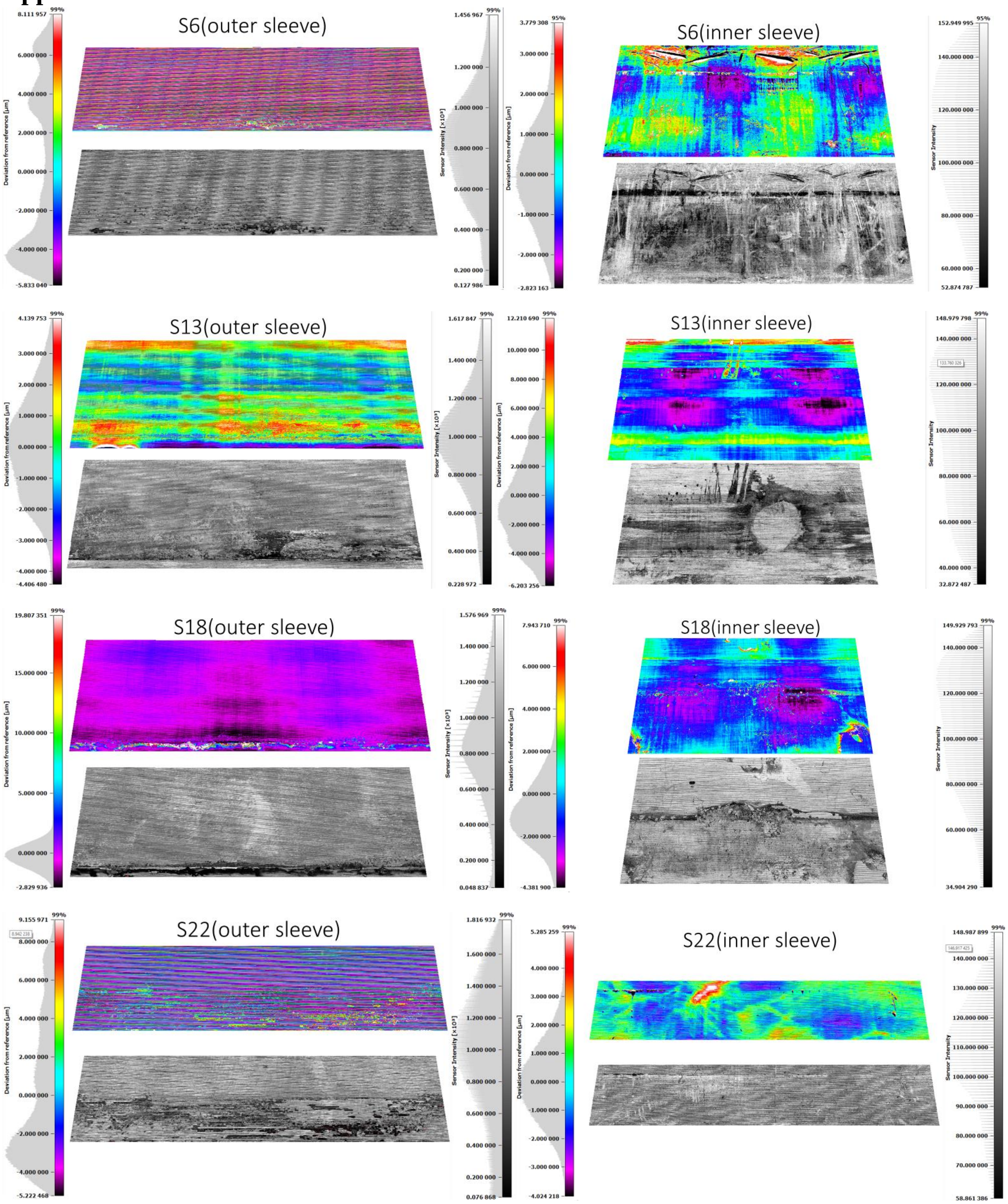

Figure 29: RedLux images for all sleeves

Appendix K

Copyright Clearance Center RightsLink®

Home | Create Account | Help

Title:	Revision total hip arthroplasty – Salvage procedures using bone allografts in Japan
Author:	Katsufumi Uchiyama,Gen Inoue,Naonobu Takahira,Masashi Takaso
Publication:	Journal of Orthopaedic Science
Publisher:	Elsevier
Date:	July 2017

ELSEVIER

LOGIN

If you're a copyright.com user, you can login to RightsLink using your copyright.com credentials.

Already **a RightsLink user** or want to learn more?

Creative Commons Attribution-NonCommercial-No Derivatives License (CC BY NC ND)

This article is published under the terms of the Creative Commons Attribution-NonCommercial-No Derivatives License (CC BY NC ND).
For non-commercial purposes you may copy and distribute the article, use portions or extracts from the article in other works, and text or data mine the article, provided you do not alter or modify the article without permission from Elsevier. You may also create adaptations of the article for your own personal use only, but not distribute these to others. You must give appropriate credit to the original work, together with a link to the formal publication through the relevant DOI, and a link to the Creative Commons user license above. If changes are permitted, you must indicate if any changes are made but not in any way that suggests the licensor endorses you or your use of the work.

Permission is not required for this non-commercial use. For commercial use please continue to request permission via Rightslink.

BACK | CLOSE WINDOW

Figure 30: Republication permission for Figure 1a

Appendix L

WOLTERS KLUWER HEALTH, INC. LICENSE TERMS AND CONDITIONS

Mar 08, 2019

This Agreement between Kirsten Sipek ("You") and Wolters Kluwer Health, Inc. ("Wolters Kluwer Health, Inc.") consists of your license details and the terms and conditions provided by Wolters Kluwer Health, Inc. and Copyright Clearance Center.

License Number	4544300112049
License date	Mar 08, 2019
Licensed Content Publisher	Wolters Kluwer Health, Inc.
Licensed Content Publication	Clinical Orthopaedics and Related Research
Licensed Content Title	Ceramic Bearings for Total Hip Arthroplasty Have High Survivorship at 10 Years
Licensed Content Author	James D'Antonio, William Capello, and Marybeth Naughton
Licensed Content Date	Feb 1, 2012
Licensed Content Volume	470
Licensed Content Issue	2
Type of Use	Dissertation/Thesis
Requestor type	Individual
STM publisher name	
Portion	Figures/table/illustration
Number of figures/tables/illustrations	1
Figures/tables/illustrations used	Figure 1
Author of this Wolters Kluwer article	No
Title of your thesis / dissertation	Ceramic Heads in Total Hip Replacements: Surgical Impaction Force and Retrieved Implant Damage Assessment
Expected completion date	Mar 2019
Estimated size(pages)	60
Requestor Location	Kirsten Sipek 35 W Central Ave LOMBARD, IL 60148 United States Attn: Kirsten Sipek
Publisher Tax ID	13-2932696
Billing Type	Invoice
Billing Address	Kirsten Sipek 35 W Central Ave LOMBARD, IL 60148 United States Attn: Kirsten Sipek
Total	0.00 USD
Terms and Conditions	

Appendix L (continued)

Wolters Kluwer Health Inc. Terms and Conditions

1. **Duration of License:** Permission is granted for a one time use only. Rights herein do not apply to future reproductions, editions, revisions, or other derivative works. This permission shall be effective as of the date of execution by the parties for the maximum period of 12 months and should be renewed after the term expires.
   i. When content is to be republished in a book or journal the validity of this agreement should be the life of the book edition or journal issue.
   ii. When content is licensed for use on a website, internet, intranet, or any publicly accessible site (not including a journal or book), you agree to remove the material from such site after 12 months, or request to renew your permission license
2. **Credit Line:** A credit line must be prominently placed and include: For book content: the author(s), title of book, edition, copyright holder, year of publication; For journal content: the author(s), titles of article, title of journal, volume number, issue number, inclusive pages and website URL to the journal page; If a journal is published by a learned society the credit line must include the details of that society.
3. **Warranties:** The requestor warrants that the material shall not be used in any manner which may be considered derogatory to the title, content, authors of the material, or to Wolters Kluwer Health, Inc.
4. **Indemnity:** You hereby indemnify and hold harmless Wolters Kluwer Health, Inc. and its respective officers, directors, employees and agents, from and against any and all claims, costs, proceeding or demands arising out of your unauthorized use of the Licensed Material
5. **Geographical Scope:** Permission granted is non-exclusive and is valid throughout the world in the English language and the languages specified in the license.
6. **Copy of Content:** Wolters Kluwer Health, Inc. cannot supply the requestor with the original artwork, high-resolution images, electronic files or a clean copy of content.
7. **Validity:** Permission is valid if the borrowed material is original to a Wolters Kluwer Health, Inc. imprint (J.B Lippincott, Lippincott-Raven Publishers, Williams & Wilkins, Lea & Febiger, Harwal, Rapid Science, Little Brown & Company, Harper & Row Medical, American Journal of Nursing Co, and Urban & Schwarzenberg - English Language, Raven Press, Paul Hoeber, Springhouse, Ovid), and the Anatomical Chart Company
8. **Third Party Material:** This permission does not apply to content that is credited to publications other than Wolters Kluwer Health, Inc. or its Societies. For images credited to non-Wolters Kluwer Health, Inc. books or journals, you must obtain permission from the source referenced in the figure or table legend or credit line before making any use of the image(s), table(s) or other content.
9. **Adaptations:** Adaptations are protected by copyright. For images that have been adapted, permission must be sought from the rightsholder of the original material and the rightsholder of the adapted material.
10. **Modifications:** Wolters Kluwer Health, Inc. material is not permitted to be modified or adapted without written approval from Wolters Kluwer Health, Inc. with the exception of text size or color. The adaptation should be credited as follows: Adapted with permission from Wolters Kluwer Health, Inc.: [the author(s), title of book, edition, copyright holder, year of publication] or [the author(s), titles of article, title of journal, volume number, issue number, inclusive pages and website URL to the journal page].
11. **Full Text Articles:** Republication of full articles in English is prohibited.
12. **Branding and Marketing:** No drug name, trade name, drug logo, or trade logo can be included on the same page as material borrowed from *Diseases of the Colon & Rectum, Plastic Reconstructive Surgery, Obstetrics & Gynecology (The Green Journal), Critical Care Medicine, Pediatric Critical Care Medicine, the American Heart Association publications and the American Academy of Neurology publications.*
13. **Open Access:** Unless you are publishing content under the same Creative Commons license, the following statement must be added when reprinting material in Open Access journals: "The Creative Commons license does not apply to this content. Use of the material in any format is prohibited without written permission from the publisher, Wolters Kluwer Health, Inc. Please contact permissions@lww.com for further information."
14. **Translations:** The following disclaimer must appear on all translated copies: Wolters Kluwer Health, Inc. and its Societies take no responsibility for the accuracy of the translation from the published English original and are not liable for any errors which may occur.
15. **Published Ahead of Print (PAP):** Articles in the PAP stage of publication can be cited using the online publication date and the unique DOI number.
   i. Disclaimer: Articles appearing in the PAP section have been peer-reviewed and accepted for publication in the relevant journal and posted online before print publication. Articles appearing as PAP may contain statements, opinions, and information that have errors in facts, figures, or interpretation. Any final changes in manuscripts will be made at the time of print publication and will be reflected in the final electronic version of the issue. Accordingly, Wolters Kluwer Health, Inc., the editors, authors and their respective employees are not responsible or liable for the use of any such inaccurate or misleading data, opinion or information contained in the articles in this section.

Appendix L (continued)

16. **Termination of Contract:** Wolters Kluwer Health, Inc. must be notified within 90 days of the original license date if you opt not to use the requested material.
17. **Waived Permission Fee:** Permission fees that have been waived are not subject to future waivers, including similar requests or renewing a license.
18. **Contingent on payment:** You may exercise these rights licensed immediately upon issuance of the license, however until full payment is received either by the publisher or our authorized vendor, this license is not valid. If full payment is not received on a timely basis, then any license preliminarily granted shall be deemed automatically revoked and shall be void as if never granted. Further, in the event that you breach any of these terms and conditions or any of Wolters Kluwer Health, Inc.'s other billing and payment terms and conditions, the license is automatically revoked and shall be void as if never granted. Use of materials as described in a revoked license, as well as any use of the materials beyond the scope of an unrevoked license, may constitute copyright infringement and publisher reserves the right to take any and all action to protect its copyright in the materials.
19. **STM Signatories Only:** Any permission granted for a particular edition will apply to subsequent editions and for editions in other languages, provided such editions are for the work as a whole in situ and do not involve the separate exploitation of the permitted illustrations or excerpts. Please view: STM Permissions Guidelines
20. **Warranties and Obligations:** LICENSOR further represents and warrants that, to the best of its knowledge and belief, LICENSEE's contemplated use of the Content as represented to LICENSOR does not infringe any valid rights to any third party.
21. **Breach:** If LICENSEE fails to comply with any provisions of this agreement, LICENSOR may serve written notice of breach of LICENSEE and, unless such breach is fully cured within fifteen (15) days from the receipt of notice by LICENSEE, LICENSOR may thereupon, at its option, serve notice of cancellation on LICENSEE, whereupon this Agreement shall immediately terminate.
22. **Assignment:** License conveyed hereunder by the LICENSOR shall not be assigned or granted in any manner conveyed to any third party by the LICENSEE without the consent in writing to the LICENSOR.
23. **Governing Law:** The laws of The State of New York shall govern interpretation of this Agreement and all rights and liabilities arising hereunder.
24. **Unlawful:** If any provision of this Agreement shall be found unlawful or otherwise legally unenforceable, all other conditions and provisions of this Agreement shall remain in full force and effect.

For Copyright Clearance Center / RightsLink Only:

1. **Service Description for Content Services:** Subject to these terms of use, any terms set forth on the particular order, and payment of the applicable fee, you may make the following uses of the ordered materials:
   i. **Content Rental:** You may access and view a single electronic copy of the materials ordered for the time period designated at the time the order is placed. Access to the materials will be provided through a dedicated content viewer or other portal, and access will be discontinued upon expiration of the designated time period. An order for Content Rental does not include any rights to print, download, save, create additional copies, to distribute or to reuse in any way the full text or parts of the materials.
   ii. **Content Purchase:** You may access and download a single electronic copy of the materials ordered. Copies will be provided by email or by such other means as publisher may make available from time to time. An order for Content Purchase does not include any rights to create additional copies or to distribute copies of the materials

Other Terms and Conditions:
v1.18

Questions? customercare@copyright.com or +1-855-239-3415 (toll free in the US) or +1-978-646-2777.

Figure 31: Republication permission for Figure 1b

VITA

KIRSTEN SIPEK

EDUCATION

MS University of Illinois at Chicago, Bioengineering May 2019

BS University of Wisconsin-Milwaukee, Civil Engineering December 2016
Minor: Spanish

WORK EXPERIENCE

Rush University Department of Orthopedics, Chicago, IL 2018-2019
Volunteer Research Assistant

- Studying failure modes of retrieved hip implants with ceramic femoral heads
- Measuring surgeon impaction force during implant placement

David's Bridal, Lombard, IL 2016 to Present
Lead Customer Service Representative

- Count inventory and receive packages
- Schedule appointments, answer phone inquiries, greet and assist customers

Village of Lisle Public Works, Lisle, IL May 2016 to August 2016
Civil Engineering Intern

- Took measurements of street patching and used construction plans to determine stationing locations
- Oversaw construction as Village representative and created daily inspection reports
- Interpreted construction plans to determine tons of asphalt needed for street resurfacing
- Created spreadsheets for sewer and pipeline locations throughout the Village

HONORS AND AWARDS

Best Graduate Author, UIC Bioengineering Student Journal 2018

1st Place Student Research Presentation, Biomedical Implant Course 2017

PUBLICATIONS

Sipek KT, Lyvers ME and Mathew MT. Failure Causes in Total Hip Replacements: A Review. Austin J Orthopade & Rheumatol. 2018; 5(1): 1064.

Sipek, K. Spine Implants: Material Selection to Avoid Failure. UIC Bioengineering Student Journal 2018; 9(1): 13-17.

PRESENTATIONS

Poster Presentation, "Surgical Impaction Force During Total Hip Arthroplasty: Effect of Material and Experience Level", Rush University Forum for Research and Clinical Investigation, March 20-21, 2019

PROFESSIONAL AFFILIATIONS

- Tau Beta Pi, 2015-Present
- Society of Women Engineers, 2012-Present

PROFESSIONAL SERVICE

Peer-Reviewed Articles for:

- Journal of Bio and Tribocorrosion

COMPUTER SKILLS

- RedLux Profiler
- ANSYS
- AutoCAD
- MatLab
- SAP 2000